ISTANBUL TECHNICAL UNIVERSITY ★ GRADUATE SCHOOL OF SCIENCE ENGINEERING AND TECHNOLOGY

NEW APPROACHES FOR THE PREPARATION OF POLYMER/CLAY NANOCOMPOSITES

Ph. D.THESIS

Muhammed AYDIN

Department of Chemistry

Chemistry Programme

MAY 2015

ISTANBUL TECHNICAL UNIVERSITY ★ GRADUATE SCHOOL OF SCIENCE ENGINEERING AND TECHNOLOGY

NEW APPROACHES FOR THE PREPARATION OF POLYMER/CLAY NANOCOMPOSITES

Ph. D. THESIS

Muhammed AYDIN
(509092215)

Department of Chemistry

Chemistry Programme

Thesis Advisor: Prof. Dr. Yusuf YAĞCI

MAY 2015

İSTANBUL TEKNİK ÜNİVERSİTESİ ★ FEN BİLİMLERİ ENSTİTÜSÜ

POLİMER/KİL NANOKOMPOZİTLERİN HAZIRLANMASINDA YENİ YÖNTEMLER

DOKTORA TEZİ

Muhammed AYDIN
(509092215)

Kimya Anabilim Dalı

Kimya Programı

Tez Danışmanı: Prof. Dr. Yusuf YAĞCI

MAYIS 2015

Muhammed AYDIN, **a Ph.D.** student of ITU **Graduate School of Science Engineering and Technology** student ID 509092215, successfully defended the **thesis** entitled "**NEW APPROACHES FOR THE PREPARATION OF POLYMER/CLAY NANOCOMPOSITES**", which he prepared after fulfilling the requirements specified in the associated legislations, before the jury whose signatures are below.

Thesis Advisor :	**Prof. Dr. Yusuf YAĞCI** İstanbul Technical University	.....
Jury Members :	**Prof. Dr. Okan SİRKECİOĞLU** İstanbul Technical University	.....
	Prof. Dr. Oya ATICI İstanbul Technical University	.....
	Assoc. Prof. Dr. M. Atilla TAŞDELEN Yalova University	.....
	Prof.Dr. Mehmet EROĞLU Marmara University	.....

Date of Submission : 9 April 2015
Date of Defense : 13 May 2015

To my mother and father

FOREWORD

First of all, I would like to thank my thesis supervisor, Prof. Yusuf YAĞCI, for giving me the opportunity without football skills to work in his group. I am deeply indebted to him for his kind guidance, support, understanding, encouragements and help in academic and social life. Without his thoroughness and help, I would have never been able to accomplish the work of my graduate research. Always, I will remember his advice "You should be best whatever you do even playing a game"
Also i would like to many thanks the Assoc. Prof. Dr. Mehmet Atilla Taşdelen, without his knowledge and excellent skills, writing of this thesis would never be possible.
I would like to thank Prof. Dr. Okan Sirkecioğlu for serving as my doctoral committee member and making valuable suggestions.
Also I acknowledge to Prof. Dr. Keriman Günaydın for her encouragements, support and guidance during my education
I would also like to express my deep thanks to all the past and present members of "Yagci Group" for their help, friendship and the nice environment they created not only inside, but also outside the lab. In particular, Ali Görkem Yılmaz, Assist. Prof. Dr. Muhammet U. Kahveci, Assist. Prof. Dr. Binnur Aydoğan, Assoc. Prof. Dr. Baris Kiskan, Dr. Ömer Suat Taskin, Gökhan Açık, Çağatay Altınkok, Cansu Aydoğan, Faruk Oytun, Senem Körk, Manolya Kukut, Cemil Dizman, Dr. Kübra Demir, Mustafa Arslan, Hüseyin Akbulut, Elyesa Murtezi, Abdurrahman Musa, Sajjad Dadashi, Dr. Sean Doran, Semih Erdur, Betül Hanbeyoğlu, Umut Uğur Özköse, Merve Kara and Ozde Yetiskin with all of you, it has really been a great pleasure.

I wish to express my warm thanks to my friends, Mustafa Çiftçi, Dr. Demet Çolak, Dr. Abdullah Aydoğan, Assist. Prof. Dr. Murat Ozmen, Metin Dağdevren, Erol Artkıy, Ozlem Kale, Assist. Prof. Dr Ferah Calisir, Assoc. Prof. Dr. M. Ali Kaplan, Mustafa Yilmaz, Hasan İsler, Kadir Danacioglu for always being next to me.

Finally, during all stages involved in the preparation of this thesis, I'm grateful to my mother Semiha and father Mehmet Ali, my brothers Yusuf, Ismail and Ahmed Aydin and sister Şüheda Aydın for their encouragement, understanding, patience and support all through my education.

MAY 2015 Muhammed AYDIN
(M.Sc. Chemist)

TABLE OF CONTENTS

Page

FOREWORD ..... **ix**
TABLE OF CONTENTS ..... **xi**
ABBREVIATIONS ..... **xiii**
LIST OF TABLES ..... **xv**
LIST OF FIGURES ..... **xvii**
SUMMARY ..... **xix**
ÖZET ..... **xxiii**
1. INTRODUCTION **1**
1.1 Purpose of Thesis 4
2. POLYSTYRENE/CLAY NANOCOMPOSITES BY ATOM TRANSFER RADICAL NITROXIDE COUPLING CHEMISTRY **7**
2.1 Experimental 12
2.1.1 Materials 12
2.1.2 Preparation of organically modified clay (T-MMT) 13
2.1.3 Preparation of polystyrene by ATRP (PSt-Br) 13
2.1.4 Synthesis of polystyrene/MMT nanocomposites (NC-1, NC-3 and NC-5) via ATRNC Chemistry 13
2.1.5 Characterization 14
3. IN-SITU SYNTHESIS OF A_3-TYPE STAR POLYMER/CLAY NANOCOMPOSITES BY ATOM TRANSFER RADICAL POLYMERIZATION **15**
3.1 Experimental 16
3.1.1 Materials 16
3.1.2 Synthesis of trifunctional ATRP initiator (Tris-ATRP initiator) 17
3.1.3 Synthesis of quaternary trifunctional ATRP initiator (Q-tris-ATRP initiator) 17
3.1.4 Preparation of organically modified clay (O-MMT) 17
3.1.5 Synthesis of A_3-type star polymer/clay nanocomposites 18
3.1.6 Characterization 18
3.2 Results and Discussion 19
3.3 Conclusions 27
4. POLYMER/CLAY NANOCOMPOSITES THROUGH MULTIPLE HYDROGEN-BONDING INTERACTIONS **29**
4.1 Experimental 31
4.1.1 Materials 31
4.1.2 Synthesis of 2-(6-isocyanatohexylamino carbonylamino)-6-methyl 4[1H] pyrimidinone (UPy-isocyanate) 31
4.1.3 Synthesis of UPy-end functionalized poly(ethylene glycol) (PEG-UPy) . 32
4.1.4 Synthesis of monohydroxytelechelic poly(ε-caprolactone) 32
4.1.5 Synthesis of UPy-end functionalized poly(ε-caprolactone) (PCL-UPy) .. 33

4.1.6 Modification of MMT-$(CH_2CH_2OH)_2$ with UPy-isocyanate (UPy-MMT) 34
4.1.7 Preparation of polymer/MMT nanocomposites by UPy-based hydrogen-bonding system 34
4.1.8 Characterization 34
4.2 Results and Discussion 35
4.2.1 Synthesis and characterization of UPy-end functionalized polymers 35
4.2.2 Functionalization of organomodified nanoclay with UPy-isocyanate. 36
4.2.3 Preparation of polymer/MMT nanocomposites by UPy-based hydrogen-bonding system 37
4.2.4 The morphology of PEG/MMT and PCL/MMT nanocomposites 40
4.2.5 Thermal behavior 42
4.3 Conclusions 45
5. CONCLUSIONS 47
REFERENCES 49
CURRICULUM VITAE 57

ABBREVIATIONS

ATRP	**:** Atom Transfer Radical Polymerization
ATNRC	**:** Atom Transfer Nitroxy Radical Coupling
$CDCl_3$	**:** Deuterated Chloroform
CH_2Cl_2	**:** Dichloromethane
CRP	**:** Controlled Radical Polymerization
CuAAC	**:** Copper Catalyzed Azide-Alkyne Cycloaddition
DMF	**:** *N*,*N*-dimehthylformamide
DMSO	**:**Dimethyl Sulphoxide
DSC	**:** Differential Scanning Calorimetry
EtOAc	**:** Ethyl Acetate
FT-IR	**:** Fourier Transform Infrared Spectrophotometer
GPC	**:** Gel Permeation Chromatography
^{1}H NMR	**:** Hydrogen Nuclear Magnetic Resonance Spectroscopy
MMA	**:**Methyl methacrylate
MMT	**:** Montmorillonite
PCL	**:** Poly(ε-caprolactone)
PEG	**:** Poly(ethylene glycol)
PMDETA	**:** *N, N, N',N'', N''*- Pentamethyldiethylenetriamine
PMMA	**:**Poly(methyl methacrylate)
PSt	**:** Polystyrene
ROP	**:** Ring-opening Polymerization
St	**:** Styrene
TEA	**:** Triethylamine
TGA	**:** Thermogravimetric Analysis
TEM	**:**Transmission Electron Microscopy
TEMPO	**:**2, 2, 6, 6-Tetramethyl-1-piperidinyloxy
THF	**:** Tetrahydrofuran
XRD	**:** X-ray Diffraction Spectroscopy
UPy	**:**2-ureido-4[1H]pyrimidinone

LIST OF TABLES

Page

Table 2.1 : Physical properties of PSt/MMT nanocomposites and their components for comparison. 9
Table 3.1 : ATRP of methyl methacrylate in the presence of different amount organophilic clay. 23
Table 3.2 : Physical properties of PMMA/MMT nanocomposites and their components for comparison. 26
Table 4.1 : Physical properties of PEG/MMT and PCL/MMT nanocomposites and their components for comparison. 40

LIST OF FIGURES

Page

Figure 1.1 : Effects of nanoparticles on various properties of polymers 2
Figure 1.2 : Preparation of polymer/clay nanocomposites by in-situ polymerization method 4
Figure 2.1 : Preparation of PSt/MMT nanocomposites by ATRNC chemistry. 9
Figure 2.2 : X-ray diffractions of Na-MMT, T-MMT and all nanocomposites. 10
Figure 2.3 : TEM micrographs showing exfoliated/intercalated silicate layers in NC-1 (A) and NC-5 (B) samples at 10 nm magnifications. 11
Figure 2.4 : TGA thermograms of Na-MMT, T-MMT, PSt-Br and PSt/MMT nanocomposites. 12
Figure 3.1 : Synthesis of quaternized tri-functional ATRP initiator (Q-tris-ATRP initiator) 19
Figure 3.2 : ^{1}H-NMR spectrum ofQ-tris-ATRP initiator 19
Figure 3.3 : FT-IR spectra ofQ-tris-ATRP initiator and organo-modified montmorillonite clay 20
Figure 3.4 : TGA thermograms of sodium and organo-modified montmorillonite clays 21
Figure 3.5 : ATRP of methyl methacrylate ($[MMA]_0/[R\text{-}X]_0/[Cu^{I}Br]_0/[L]_0$ = 100/1/3/3), a) kinetic plot and b) molecular molecular weights and distributions of resulting polymers as a function of degree of conversion. 22
Figure 3.6 : X-ray diffractions of Na-MMT, O-MMT and obtained nanocomposites (NC-1, 3, 6 and 10). 23
Figure 3.7 : TEM micrographs showing exfoliated/intercalated silicate layers in NC-1 (a), NC-3 (b), NC-6 (c) and NC-10 (d) samples at higher magnification (scale bar: 20 nm). 25
Figure 3.8 : TGA thermograms of A_3-PMMA and PMMA/MMT nanocomposites (NC-1, 3, 6 and 10). 26
Figure 3.9 : DSC traces of A_3-PMMA star polymer and PMMA/MMT nanocomposites (NC-1, 3, 6 and 10). 27
Figure 4.1 : Synthesis of UPy-PEG and UPy-PCL monotelechelics. 35
Figure 4.2 : Functionalization of MMT-$(CH_2CH_2OH)_2$ with UPy-isocyanate. 36
Figure 4.3 : Preparation of PEG/MMT and PCL/MMT nanocomposites 38
Figure 4.4 : FT-IR spectra ofneat PEG-UPy, MMT-UPy and PEG/MMT-20 nanocomposite 38
Figure 4.5 : FT-IR spectra ofneat PCL-UPy, MMT-UPy and PCL/MMT-20 nanocomposite 39
Figure 4.6 : TEM micrographs of PEG/MMT-5 in low (a, scale bar: 200 nm) and high (b, scale bar: 20 nm) magnifications. 41
Figure 4.7 : TEM micrographs of PCL/MMT-5 in high (scale bar: 20 nm) magnification. 42

Figure 4.8 : TGA thermograms of neat PEG-UPy and resulting nanocomposites containing 3, 5, 10 and 20 % MMT-UPy.....43
Figure 4.9 : TGA thermograms of neat PCL-UPy and resulting nanocomposites containing 3, 5, 10 and 20 % MMT-UPy.....44
Figure 4.10 :DSC traces of a) neat PEG-UPy and resulting nanocomposites b) neat PCL-UPy and resulting nanocomposites.....45

NEW APPROACHES FOR THE PREPARATION OF POLYMER/CLAY NANOCOMPOSITES

SUMMARY

Polymer/clay nanocomposites have exhibited immensely enhanced properties and higher performance as compared to both their conventional polymer composites and pure polymers. Currently polymer/clay nanocomposites can be prepared by three ways such as solution mixing, melt blending, and *in-situ* polymerization. Solution mixing method consists to solubilize polymer in an organic solvent, then the clay is dispersed in the obtained solution and subsequently either the solvent is evaporated or the polymer precipitated. The large quantities of volatile solvent necessary for this approach make it less attractive as an industrial process. Melt blending is a solvent-free method to enable mixing of the layered silicate with the polymer matrix in the molten state. However, very careful attention has to be paid to finely tune the processing conditions to increase the compatibility of clay layer surfaces with the polymer matrix. In the *in-situ* polymerization technique, the monomer, together with the initiator and/or catalyst, is intercalated within the silicate layers and the polymerization is initiated by external stimulation such as thermal, photochemical or chemical activation. The chain growth in the clay galleries triggers the clay exfoliation and hence the nanocomposite formation.The in-situ polymerization can be initiated by externally stimulation such as thermal, photochemical or chemical activation. The growth of polymer chains within the clay galleries may lead to the clay exfoliation and hence the nanocomposite formation.Recently, a highly efficient method, namely copper (I) catalyzed azide/alkyne cycloaddition (CuAAC) "click" reaction, in which exfoliation is rooted in the functional groups of the intercalant that readily react with the antagonist groups of the preformed polymershas been established. To take advantage of click chemistry, azide and alkyne partners could each be incorporated in either the clay surface or polymer chain. The quantitative efficiency of coupling reaction coupled with tolerance to a wide variety of functional groups and reaction conditions make this coupling process highly attractive for the nanocomposite preparation. However, there are limited examples in the literature to date regarding the preparation of polymer/clay nanocomposites via the CuAAC click reactions.

In the first part of thesis,an efficient protocol, atom transfer radical nitroxide coupling chemistry (ATNRC), for the preparation of polymer/clay nanocomposites via grafting-onto strategy with well-defined polymer synthesized via atom transfer radical polymerization has been described. The highly efficient ATNRC chemistry was based on mixing a nitroxide-containing organoclay with corresponding halide-containing polystyrene in the presence of Cu(I)Cl/PMDETA catalytic system was developed.The radical coupling, taking place between the clay layers, not only leads to attach the polymer chain but also successful nanocomposite formation with highly exfoliated morphology (Figure 1). Spectroscopic and microscopic investigations revealed that successful nanocomposite formation has been achieved by this method.

By addition of small amounts of layered silicate loadings resulted in remarkable improvements of thermal properties of nanocomposites.

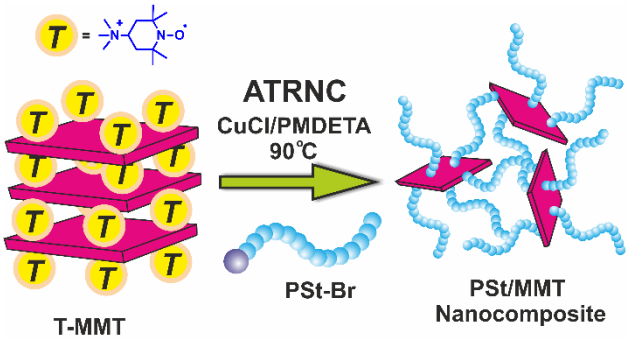

Figure 1: Preparation of polymer/clay nanocomposites by ATNRC chemistry

In the second part of thesis,a series of A_3-type star poly(methylmethacrylate)/clay nanocomposites has been prepared by *in-situ* atom transfer radical polymerization (ATRP) initiated from organomodified montmorillonite containing quaternary trifunctional ATRP initiator (Figure 2). The first order kinetic plot showed a linear behavior, indicating the controlled character of the polymerization. The resulting nanocomposites were characterized by spectroscopic, thermal and microscopic analyses. Spectroscopic and microscopic investigations revealed a complex morphology, with partial intercalation/exfoliation, which depends on the concentration of clay.The exfoliated nanocomposite was obtained when polymerization was conducted with 1% of organic clay loading.However, with increasing the clay loading to 3, 6 and 10%, the degree of exfoliation of the nanocomposites decreased, which confirmed by both spectroscopic and microscopic analyses. Thermal analyses show that all nanocomposites had higher glass transition values and thermal stabilities compared to neat polymer.

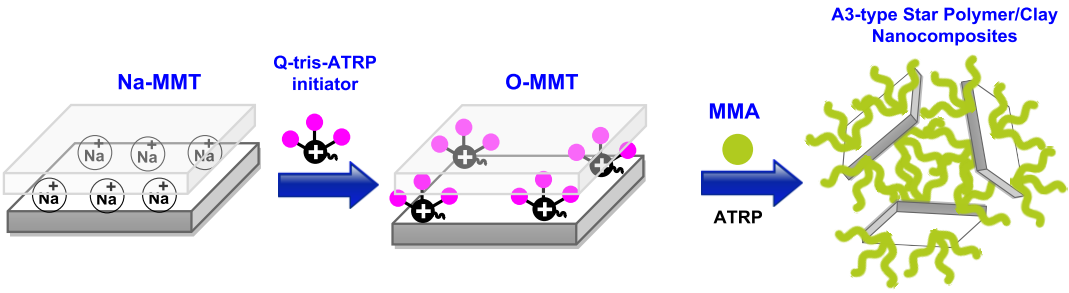

Figure 2: *In-situ* preparation of A_3-type star poly(methylmethacrylate)/clay nanocomposites by ATRP

In the third part of thesis, the preparation of polymer/clay nanocomposites by specific hydrogen bonding interactions between surface functionalized silica nanoclays and 2-ureido-4[1H]pyrimidinone-bonded supramolecular poly(ethylene glycol) or poly(ε-caprolactone)s, which has self-association capability through quadruple hydrogen bonds was described (Figure 3). An 2-ureido-4[1H]pyrimidinone (UPy) motif with self-association capability (through quadruple hydrogen bonds) was successfully anchored onto montmorillonite clay layers. Polymer/clay nanocomposites were prepared by specific hydrogen bonding interactions between surface functionalized silica nanoclays and UPy-bonded

supramolecular poly(ethylene glycol) or poly(ε-caprolactone). The mixed morphologies including intercalated layers with a non-uniform separation and exfoliated single layers isolated from any stack were determined by combined spectroscopic and microscopic analyeses. Thermal measurements showed that all nanocomposites have higher decomposition temperatures and thermal stabilities comparedto neat polymer. Thedifferential scanning calorimetry data implied that thecrystallinity of polymers did not show essential changes upon introduction of organomodified UPy clays.

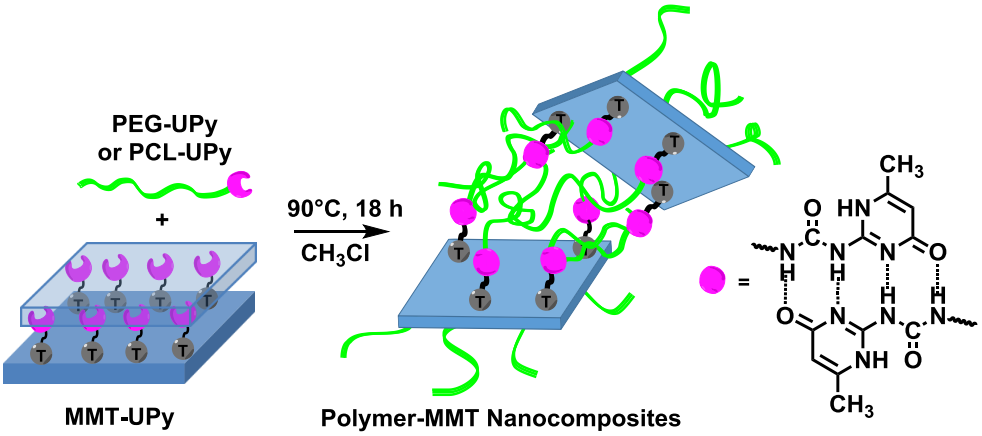

Figure 3: Preparation of polymer clay nanocomposites through multiple hydrogen-bonding interactions

POLİMER/KİL NANOKOMPOZİTLERİN HAZIRLANMASINDA YENİ YÖNTEMLER

ÖZET

Nanokompozit malzemeler üstün optik, termal, elektronik, fotonik, manyetik, reolojik, yapısal ve mekanik niteliklerinden dolayı her geçen gün kullanımı artmaktadır. Plastik sektöründe büyük paya sahip olan, otomotiv, kaplama, biyomedikal ve paketleme sanayileri en önemli kullanım alanlarıdır. Genel bir tanımla; iki veya daha fazla malzemenin, iyi özelliklerini bir araya toplamak ya da ortaya yeni bir özellik çıkarmak için, mikro veya makro seviyede heterojen karışımıyla oluşan malzemeye "kompozit malzeme" denir. Nanokompozitler, sürekli bir polimer matris içerisine dağılmış en az bir boyutu 100 nanometreden küçük olan parçacıkları içeren heterofazlı kompozit yapılardır.

Nanokompozit üretiminde kullanılan katkı maddeleri nanoyapılarına göre üç ana kategoriye ayrılmaktadır. Bunlar tek nanoboyutlu killer, iki nanoboyutlu karbon nanotüpler ve nanoteller, ve son olarakta üç nanoboyutlu silika, metal partiküller ve kuantum taneciklerdir. Polimerik kil nanokompozitlerin hazırlanmasında birçok metot geliştirilmiştir. Bu yöntemlerin bir kaçı; tabakalı killer varlığında gerçekleşen yerinde polimerizasyon (in-situ polymerization), erime ile arayı açma (melt intercalation) ve çözelti ortamında arayı açma (intercalation in solution) şeklinde sıralanmaktadır.Yerinde polimerizasyon ile polimer nanokompozit hazırlama, polimer zincirininbüyümesi ile es zamanli olarak nanokillerin dagitilmasi esasına dayanır. Bu yöntemde ilk olarak nanokiller monomer veya monomer çözeltisi ile karıştırılır ve ardından polimerizasyon ısı, radyasyon veya başlatıcı etkisi ile başlatılır. Kil tabakalari arasinda büyüyen polimer zincirleri tabakalar arası mesafelerin artması ve tabakaların oluşan polimer matris içerisinde rastgele dağıtılmasını mümkün kılmaktadır. Bu yönteminavantajlarından birisi, polimer eriği veya polimer çözeltisine nazaran daha düşükviskoziteye sahip monomer çözeltisi içerisinde bulunan nanokil tabakalarinin ultrasound veya yüksek kesme karıştırması (high shear mixing) etkisi ile dağıtılmasına olanak sağlamasıdır. Özetle, yerinde polimerizasyon yöntemi içerisinde, nanopartiküllerin moleküler ölçekte dağıldığı polimer nanokompozitlerinhazırlanmasında kullanılır. Son zamanlarda bakır (I) katalizörlu azit-alkin dipolar siklokatılma tepkimesi olarakta bilinen Click kimyasi tepkimesinde polimer/kil nanokompozitlerin hazırlanmasında kullanılmıştır. Click kimyasına uygun azit yada alkin fonksiyonlu nanokiller ile karşıt grupları içeren polimerler basit tepkime koşullarında tepkimeye sokularak polimer/kil nanokompozitler elde edilmiştir. Özellikle bir çok fonksiyonel gruplarla uyumlu olmasi ve kisa surelerde yüksek verimlerle gerçekleşmesinden dolayı Click kimyasi tepkimesi polimer/kil nanokompozit sentezleri için önemli bir yöntem olmuştur.

Bu tezin ilk bolumunde, etkili bir yontem olarak bilinen nitroksit radikal kenetlenme tepkimesiyle polimer/kil nanokompozitleri hazirlandi. Öncelikle nitroksit radikal kenetlenme tepkimesi için uygun nitroksil fonksiyonlu kil sentezlenmistir. Bunun icin sodyum montmorillonit kilinin sodyum iyonlariyla 2,2,6,6- tetrametil piperidinin

kuartenize amonyum tuzu yer degistirilerek organomodifiye kil elde edilmistir. Elde edilenfonksiyonel kilfarkli oranlarda brom uçlu polistiren ile 120 ºC'de bakır (I) bromür/N,N,N´,N´´,N´´-pentametildietilentriaminvarlığında tepkimeye sokularak polistiren/kil nanokompozitler hazirlanmistir (Sekil 1). Kil tabakalari arasinda gerceklesen nitroksit radikal kenetlenme tepkimesiyle hem polistiren zincirleri tabakalar arasina yerlestirildi hemde bu tabakalarin polimer icerisinde homojen bir bicimde dagitilmasi saglandi. Elde edilen nanokompozit malzemelerin termal ve yüzey özellikleri değişik analiz yöntemleriyle incelendi. Bu yontemlerden alinan sonuclarla tamamiyla dagitilmis yada kismi olarak dagitilmis kil nanotabakalari iceren polimer killer basariyla sentezlenmistir. Termal analiz sonuclarina gore kucuk oranlarla takviyelendirilen polimerlerin daha yuksek termal ozellikler gosterdigi gozlemlenmistir.

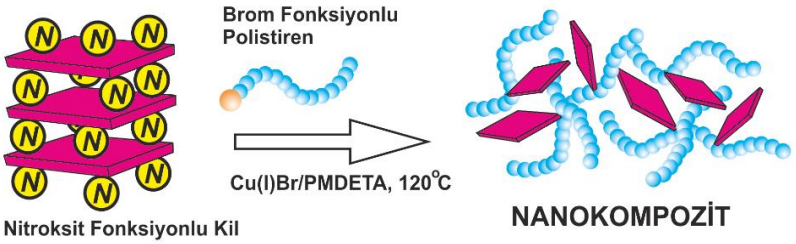

Şekil 1 : Polimer/kil nanokompozitlerin ATNRC kimyasıyla hazırlanması

Bu tezin ikinci bolumunde, atom transfer radikal polimerizasyonu (ATRP) yontemiyle A_3-tipi yildiz polimer/kil nanokompozitleri hazirlandi. Kil arasinda yildiz polimer sentezleyebilmek icin sodyum montmorillonit kilinin sodyum iyonlariyla uc fonksiyonlu ATRP baslatici iceren kuartenize amonyum tuzu yer degistirilerek organomodifiye kil hazirlanmistir. Elde edilenfonksiyonel kilfarkli oranlarda metil metakrilat monomeri varliginda ile 90 ºC'de bakır (I) bromür/N,N,N´,N´´,N´´-pentametildietilentriaminvarlığında tepkimeye sokularak polimer/kil nanokompozitler sentezlenmistir (Sekil 2). Kil tabakalari arasinda gerceklesen ATRP tepkimesinin kontrollu polimerizasyon davranisi gosterdigi gozlemlenmistir. Yapisal aydinlatma calismalari sonucu elde edilen nanokompozit malzemelertamamiyla dagitilmis yada kismi olarak dagitilmis kil nanotabakalari icerdigi bulunmustur. Dusuk oranda kille beslenen (%1 nanokil takviyeli) nanokompozitin yapisindaki kil tabakalarinin tamamiyla dagitilmis yapida oldugu hem X-Ray difraktometrei hemde gecirimli electron mikroskopu yontemiyle kanitlanmistir. Polimer icindeki nanokil oranin artisiyla yapida kismi olarak arasi acilmis (interkale olmus) kil tabakalarininda miktarinda artis oldugu gozlemlenmistir. Termal analiz sonuclarina gore saf polimere gore tum nanokompozitler daha ustun termal ozellikler gostermistir.

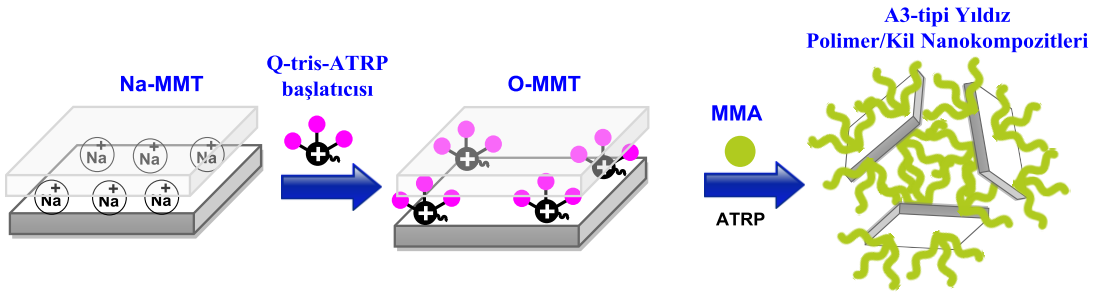

Şekil 2 : A_3-tipi yıldız polimer/kil nanokompozitlerin ATRP yöntemiyle hazırlanması

Bu tezin son bolumunde, coklu hidrojen bag etkilesimleri kullanilarak yinepolimer/kil nanokompozitleri hazirlanmistir. Bu amacla ureido-4[1H]pirimidinon (UPy) sonlu poli(etilen glikol) ve poly(ε-kaprolakton) polimerleri sentezlendi. Diger taraftan yine ureido-4[1H]pirimidinon fonksiyonlu nanokiller ticari olarak satilan ve iki adet hidroksil fonksiyonalitesi bulunan montmorillonit kili (Cloisite 30B) ile ureido-4[1H]pirimidinon-hekzametil izosiyanatin uretan bagi olusturmasiyla elde edilmistir. Daha sonra fonksiyonel nanokil ile UPy sonlu polimerler arasinda gerceklesen dortlu hidrojen koprulerinin olusumuyla hem polimer zincirleri tabakalar arasina yerlestirildi hemde bu tabakalarin polimer icerisinde homojen olarak dagitilmasi saglandi (Sekil 3). Spektroskopi ve mikroskop calismalari sonucu nanokompozit malzemelertamamiyla dagitilmis yada kismi olarak dagitilmis kil nanotabakalari iceren karisik bir yapiya sahip oldugu bulunmustur. Polimer icindeki nanokil oranin artisiyla yapida kismi olarak arasi acilmis (interkale olmus) kil tabakalarinin sayilarinda artis onceki calismalarda oldugu gozlemlenmistir. Termal analiz sonuclarina gore saf polimere gore tum nanokompozitler daha yuksek sicakliklarda bozundugu tespit edilmistir. Ayrica diferansiyel taramali kalorimetre sonuclarina gore nanokil ilavesiyle polimerlerin kristal yapilarinda bir degisiklik gozlemlenmemistir.

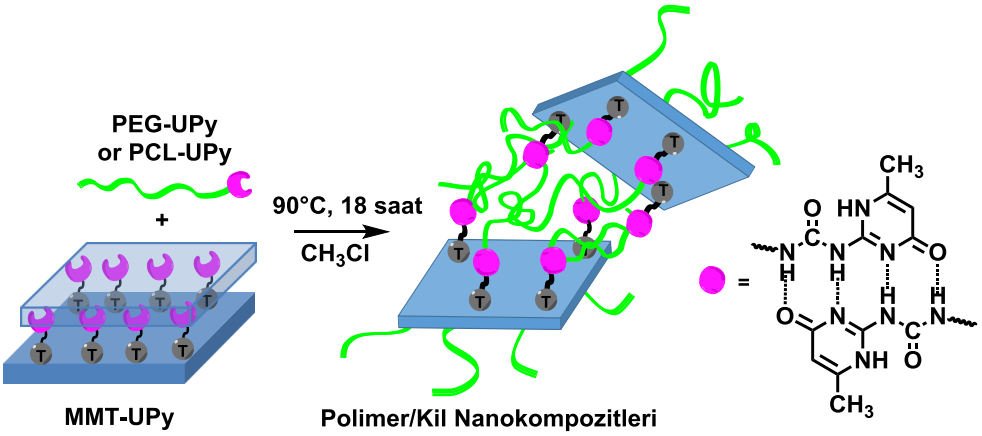

Şekil 3 : Polimer/kil nanokompozitlerin çoklu hidrojen-bağ etkileşimleriyle hazırlanması

1. INTRODUCTION

Nanotechnology is a recently established approach that provides the development of functional materials in molecular scale, starting from physical, chemical and biological matters. The future technology is predicted to be built up on the organization of the nanostructures, shape control, design and functionalization of the materials in the atomic, molecular and nanocluster scale. It is possible to obtain nanomaterials with different properties either via producing new substances by the help of nanotechnology or by using some materials already present in nature like Au, Fe_2O_3, nanoparticles in earth, clay nanolayers and zeolit. Nanomaterials display fine optical, thermal, electronical, photonic, magnetic, reological, structural and mechanical properties because of their very small sizes. The reason for this positive development in these properties can be attributed to high surface-volume ratio, limited interactions between the atoms and the molecules without volumetric behaviours and quantum effects which take place only in the nano-scale structures. Nanostructures provide production of many materials like more transparent glasses, lighter and more durable cars, cleaner clothes, longer-living paints which strongly affect our daily lives.

Nanocomposites have become a striking research area in the last decade. However, as their behaviors and properties are not clearly understood, their industrial applications are only limited to some extent. Thus, nanocomposites are the prior research and development area especially in automotive, electronic devices and food packaging industries.The incorporation of nanoparticles in polymer matrices leads to significant improvements in their physical properties as illustrated in the Figure 1.1.

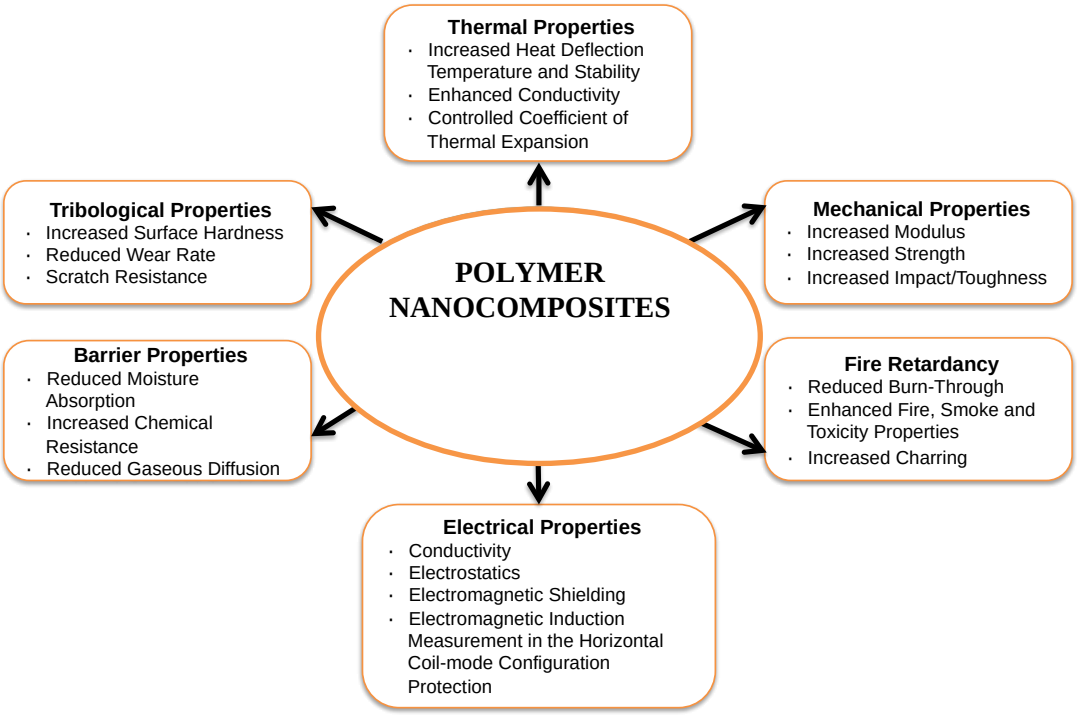

Figure 1.1 : Effects of nanoparticles on various properties of polymers

Polymer/clay nanocomposite materials, in which nano-sized silicate plates of clay are uniformly dispersed in the polymer matrix, exhibit superior physical properties such as high dimensional stability, gas barrier performance, flame retardancy, and mechanical strength that cannot be achieved by pure polymer or conventional composites (micro- and macro composites).Furthermore, polymer layered silicate nanocomposites avoid processing techniques (e.g. extrusion) which are used for materials with a higher content of reinforcement.This polymer/clay nanocomposites can be prepared in several ways, namely, solution exfoliation, melt intercalation, *in situ* polymerization and template synthesis. Solution exfoliation can be only used with water-soluble polymers to produce mostly intercalated nanocomposites, because of the need of large amounts of solvent to ensure a good clay dispersion. Melt intercalation is a solvent-free method which enables mixing of the layered silicate with the polymer matrix in the molten state. However, very careful attention has to be paid to finely tune the processing conditions to increase the compatibility of clay layer surfaces with the polymer matrix. In the *in situ* polymerization technique, the monomer, together with the initiator and/or catalyst, is intercalated within the silicate layers and the polymerization is initiated by external stimulation such as thermal, photochemical or chemical activation. The chain growth in the clay galleries triggers the clay exfoliation and hence the nanocomposite formation. Unlike melt

intercalation, the low viscosity of the monomer (if compared with the polymer) in the *in situ* polymerization makes it more easy to break up particle agglomerates by using high shear devices, resulting in a more uniform mixing of particles in the monomer. In template synthesis clay layers are formed by crystallization in an aqueous polymer gel. However, the layers show a limited length and the size are not comparable to pristine clays. Furthermore, it is possible to control nanocomposite morphology through the combination of reaction conditions and clay surface modification. Remarkable progress has been achieved in understanding the important factors in processing nanocomposites, which include clay modification, dispersion of clay particles into the reaction mixtures, its formation of ultimate clay morphology, and the concomitant effects on both reaction behavior and final composite properties.

Recently, the polymer/clay nanocomposites have been also synthesized by various *in-situ* polymerization methods such as ring-opening polymerization (ROP), controlled radical polymerization (CRP), conventional free radical polymerization, cationic polymerization, and living anionic polymerization. Although limited structural and molecular weight control is achieved, in situ conventional free radical polymerization is still the most practically applied process because of its simplicity and applicability to a wide range of monomers without any specific structural selectivity. Moreover, it does not require any additional catalysts, particularly inorganic salts, which may interfere with the intercalation.In-situ polymerization method can allow polymer molecules to grow inside the clay galleries upon irradiation and consequently form covalent bonds between organic and inorganic phases. Attachment of either initiator or monomeric sites into clay layers and subsequent polymerization of immersed monomers facilitate propagation and exfoliation processes concomitantly leading to the formation of homogenous clay-polymer nanocomposites (Figure 1.1). In order to ensure strong bonding between nanoparticles and the organic matrix, covalent bonds were utilized to incorporate clay platelets. These efforts mainly consist of surface initiated polymerization either by modifying the platelets with reactive functional groups or by modifying with initiator molecule.Although *in-situ* polymerization has proved successful in the preparation of various polymer–layered silicate nanocomposites, it has some drawbacks: (i) it is a time-consuming preparation route (the polymerization reaction may take more than 24 h); (ii) exfoliation is not always thermodynamically stable;

and the platelets may re-aggregate during subsequent processing steps; and (iii) the process is available only to the resin manufacturer who is able to dedicate a production line for this purpose.

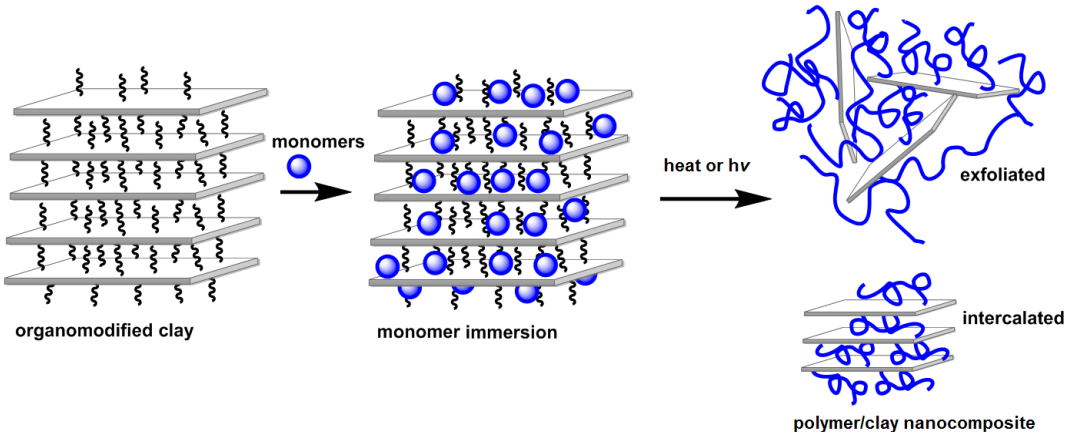

Figure 1.2 : Preparation of polymer/clay nanocomposites by in-situ polymerization method

Recently a conceptually different approach, using click chemistry,was introduced for the preparation polymer/clay nanocomposites. The click chemistry reactions are useful in attaching chains to the surface of particles, as they can be carried out withhigh efficiency under relatively mild conditions. To take advantage of click chemistry, azide and alkyne partners could each be incorporated in either the clay surface or polymer chain. The quantitative efficiency of coupling reaction coupled with tolerance to a wide variety of functional groups and reaction conditions make this coupling process highly attractive for the nanocomposite preparation.

1.1 Purpose of The Thesis

The objective of the thesis is to synthesize and study various well-defined polymernanocomposites by combination of controlled polymerization methods with click chemistry reaction or hydrogen bonding interactionsbetween surface functionalized silica nanoclays and monotelechelic polymers.During this thesis, chromatographic (GPC), spectroscopic (^{1}H-NMR, FT-IR and XRD), thermal (DSC and TGA) and microscopic (TEM) analyses are performed for the obtained nanomaterials.This thesis is organized in such that each chapter has its own introduction, experimental, results and discussion, and list of references.

Chapter 1 discusses overall background information about the development of polymer/clay nanocomposite preparation, about the traditional preparation methods and properties gains of nanoclay filled polymers, and finally about the recently developped preparation methods including click chemistry reactions.

Chapter 2 describes the synthesis of polystyrene/clay nanocomposites via a highly efficient atom transfer nitroxide radical coupling (ATNRC) chemistry which, is based on mixing a nitroxide-containing organoclay with corresponding halide-containing polystyrene in the presence of CuCl/PMDETA catalytic system.

Chapter 3 gives a detailed account of the preparation of a series of A_3-type star poly(methylmethacrylate)/clay nanocomposites via in-situ atom transfer radical polymerization initiated from organomodified montmorillonite containing quaternary trifunctional ATRP initiator.

Chapter 4 involves the synthesis and characterization of polymer/clay nanocomposites by specific hydrogen bonding interactions between surface functionalized silica nanoclays and 2-ureido-4[1H]pyrimidinone-bonded supramolecular poly(ethylene glycol) or poly(ε-caprolactone)s, which has self-association capability through quadruple hydrogen bonds.

Finally, concluding remarks are summarized in Chapter 5 along with recommendations for further work.

2. POLYSTYRENE/CLAY NANOCOMPOSITES BY ATOM TRANSFER RADICAL NITROXIDE COUPLING CHEMISTRY

During the last two decades, the introduction of well-dispersed clay layers such as montmorillonite (MMT) into a polymer matrix has been proved to be extremely effective in the improvement of mechanical, thermal and barrier properties of the polymers[1]. However, the dispersion of clay as individual platelets throughout the polymer is difficult to achieve due to strong van der Waals forces holding platelets together in conjunction with the incompatibility of the hydrophilic clay with the organophilic (hydrophobic) polymer matrix, giving way to clay agglomeration. Thus, the surface of the clays is commonly modified with a cation exchange technique to expand basal spacing and make the layered silicate compatible with polymer matrixes. Currently polymer/clay nanocomposites can be prepared by three ways such as solution mixing, melt blending, and *in-situ* polymerization[2]. In the solution mixing method, the polymer is dissolved in an organic solvent, then the clay is dispersed in the obtained solution and subsequently either the solvent is evaporated or the polymer precipitated. However, the large quantities of volatile solvent necessary for this approach make it less attractive as an industrial process. Melt blending is a solvent-free method to enable mixing of the layered silicate with the polymer matrix in the molten state. However, very careful attention has to be paid to finely tune the processing conditions to increase the compatibility of clay layer surfaces with the polymer matrix[3]. In the *in-situ* polymerization technique, the monomer, together with the initiator and/or catalyst, is intercalated within the silicate layers and the polymerization is initiated by external stimulation such as thermal, photochemical or chemical activation[4-16]. The chain growth in the clay galleries triggers the clay exfoliation and hence the nanocomposite formation.

Recently, our group has established a highly efficient method, namely copper (I) catalyzed azide/alkyne cycloaddition (CuAAC) “click” reaction[17], in which exfoliation is rooted in the functional groups of the intercalant that readily react with the antagonist groups of the preformed polymers[18-20]. To take advantage of click

chemistry, azide and alkyne partners could each be incorporated in either the clay surface or polymer chain. The quantitative efficiency of coupling reaction coupled with tolerance to a wide variety of functional groups and reaction conditions make this coupling process highly attractive for the nanocomposite preparation. However, as far as we are concerned that there arenot so many examples in the literature to date regarding the preparation of polymer/clay nanocomposites via the CuAAC click reaction[21-23].

Recently, Huang and coworkers presented a rapid, selective, and reversible atom transfer nitroxide radical coupling (ATNRC) reaction, which has the attributes of a "click" reaction with quantitative yields and high tolerance offunctional groups[24-28]. This reaction involves formation of a reactive radical by an atom transfer reaction with a copper catalyst and trapping of this radical with a persistent nitroxide radical at close to diffusion-controlled rates. Although, this strategy has been applied for the preparation of graphene-based nanocomposites[29], to the best of our knowledge, it has not been reported for polymer/clay nanocomposites in the literature. Here, we report the synthesis of polystyrene/MMT nanocomposites by ATRNC chemistry. This approach is conceived to greatly extend the synthetic capabilities of polymer/clay nanocomposites by careful choices of organic clays and polymers, and the optimization of the synthesizing process to deliver the biggest benefit.

As a highly efficient atom transfer nitroxide radical coupling (ATNRC) chemistry is based on mixing a nitroxide-containing molecule with corresponding halide-containing polymer in the presence of CuCl/PMDETA catalytic system. It can serve as a relative convenient and safe way with "click-like" efficiency to synthesize the certain macromolecular structures with well-defined properties. For this purpose, a quaternized ammonium-containing TEMPO was first synthesized from 4-dimethylamino-TEMPO and methyl bromide[30], then ion-exchanged with sodium montmorillonite (Na-MMT) to obtain TEMPO containing organomodified clay (T-MMT). Gallery distances (basal space, d_{001}) of pure clay and organomodified-clay (Na-MMT and T-MMT) were determined by X-ray diffraction (XRD) analysis (Figure 2.2 and Table 2.1). The pristine clay sample (Na-MMT) exhibited a peak at 9.80° (Figure 2.2 bottom), which corresponded to d_{001} of 0.90 nm and this peak shifted to 7.82° for T-MMT, which corresponded to d_{001} of 1.12 nm. This change indicated that the T-MMT was successfully intercalated into the silicate galleries of

the MMT clay. The mass loss of T-MMT was 21.4%; it indicated that the percent of attached TEMPO was 13% (Table 2.1). Larger interlayer spaces not only help the diffusion of polymer chains, but also assist the exfoliation of silicate layers by providing more hydrophobic environment. The bromide-functionalized polystyrene (PSt-Br) was synthesized by typical ATRP using ethyl-2-bromopropionate as initiator and CuCl/PMDETA as catalyst. The low-conversion (21%) and low-molecular-weight polymer (M_n = 2300, M_w/M_n = 1.12) was prepared in order to perform successful coupling process.

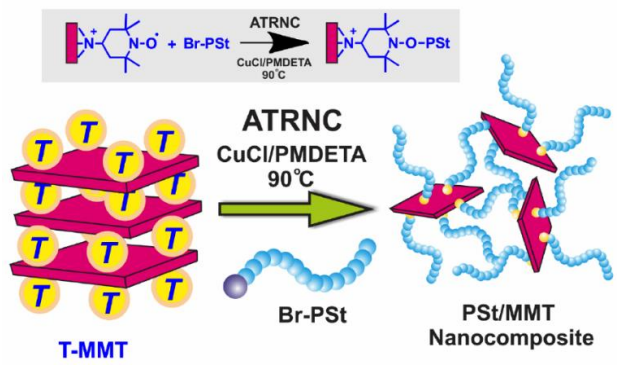

Figure 2.1 : Preparation of PSt/MMT nanocomposites by ATRNC chemistry.

A series of PSt/MMT nanocomposites (NC-1, NC-3 and NC-5) were prepared by ATNRC reaction between PSt-Br and T-MMT in the presence of CuCl/PMDETA using toluene as solvent at 90 °C and the results were summarized in Table 2.1. The coupling efficiencies of ATNRC were higher than 90%, which is similar to that of click chemistry.

Table 2.1 : Physical properties of PSt/MMT nanocomposites and their components for comparison.

Entry	Clay (%)	Conversion[a]	d_{001}[b] (nm)	Tg[c] (°C)	Weight loss Temperature[c](°C)		Char Yield[c] (%)
					%10	%50	
Na-MMT	-	-	0.90	-	-	-	91.6
T-MMT	-	-	1.12	-	498	-	78.6
PSt-Br	-	-	-	93	290	348	<1
NC-1	1	91	-	96	292	385	8.2
NC-3	3	93	1.43	101	304	393	11.9
NC-5	5	96	1.50	105	343	400	14.1

[a] Determined by gravimetrically. [b] Basal spacing (d_{001}) is calculated by XRD analysis. [c] Determined by DSC and analyses under a nitrogen flow at a heating rate of 10 °C/min.

Figure 2.2 shows the XRD patterns of PSt/MMT nanocomposites with the MMT contents of PSt-MMT- 1%, 3%, 5% and pure T-MMT. The characteristic peak of the T-MMT disappears in the X-ray diffraction patterns of PSt-MMT-1% nanocomposite (NC-1), which indicates the formation of exfoliated structure of clay. However, it was found that partially exfoliated or intercalated structures existed in the high clay content system (PSt-MMT-3% and 5%) probably due to the difficulty for overcoming the intensive ionic attraction between the neighboring platelets.

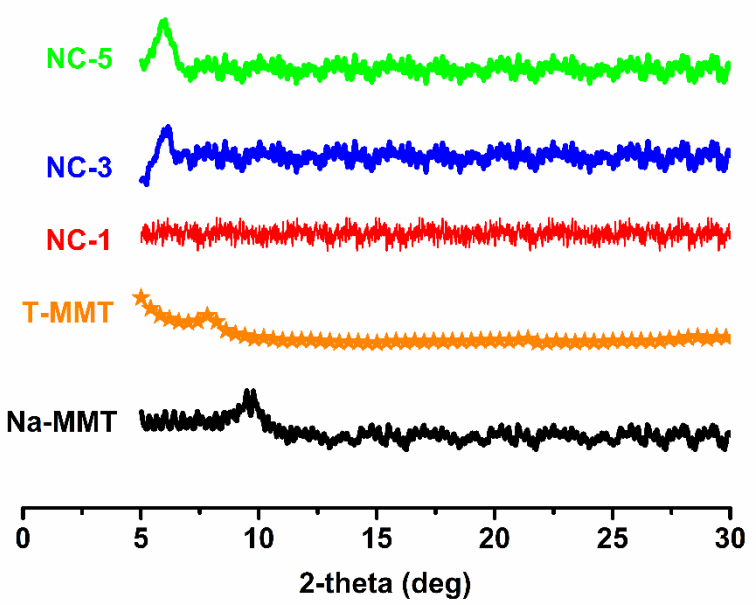

Figure 2.2 : X-ray diffractions of Na-MMT, T-MMT and all nanocomposites.

Although XRD offers a convenient and practical method to determine the interlayer spacing, it cannot be used alone as a criterion for exfoliation. Several factors such as clay dilution, peak broadening and preferred orientation make XRD characterization of nanocomposite susceptible to errors. Thus, TEM studies are necessary to verify the dispersion of silicate layers in the polymer matrix and exfoliation achieved. Figure 2.3 presents the high magnification transmission electron microscope (TEM) images of PSt/MMT nanocomposites containing 1.0 and 5.0 wt % T-MMT, respectively. The dark lines represent the clay nanolayers, whereas the gray areas correspond to the PSt matrix. The images clearly revealed that some of silicate layers were dispersed uniformly, indicating most of the silicate layers were exfoliated. But in some areas, intercalated layers with a size of 50-100 nm were also observed. Combined together with the results of XRD and TEM, it can be concluded that an exfoliated and intercalated structure co-exists (also called incomplete exfoliation) in the nanocomposites.

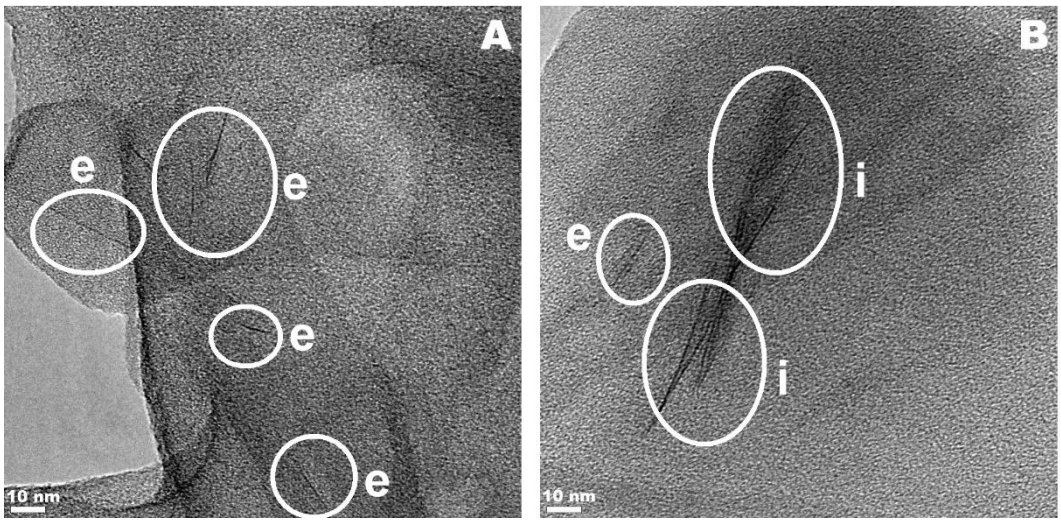

Figure 2.3 : TEM micrographs showing exfoliated/intercalated silicate layers in NC-1 (A) and NC-5 (B) samples at 10 nm magnifications.

The thermogravimetric analysis (TGA) curves of pure polymer and PSt/MMT nanocomposite recorded in inert atmosphere are shown in Figure 2.4. As indicated in the figure, the thermal behavior of the nanocomposite is quite similar to the pure polymer and single step decomposition is observed for all the samples. The values of onset (T_{10}) and midpoint (T_{50}) degradation temperatures are compared in Table 2.1. It can be clearly found that both degradation temperatures of the nanocomposites shifted significantly toward higher temperatures compared to those of the neat PSt. These improvements could be associated with the clay as an inorganic material with high thermal stability and great barrier properties that can prevent the heat from transmitting quickly and can limit the continuous decomposition. As the clay contents increases from 1 to 5 wt%, the increase of 8.2-14.1% of the char residue is also observed, which means that the silicate layers can promote the charring process during the decomposition process. The increase in char yield implies good thermal stability. According to the differential scanning calorimetry (DSC) characterization, the glass transition temperature of the nanocomposites increased with the clay content by a maximum of 12 ^{o}C (Table 2.1).). The polystyrene chains were physically linked to the clay plates. This effect limited the movement of the polymer chains and resulted an increase the glass transition temperature of the polystyrene.

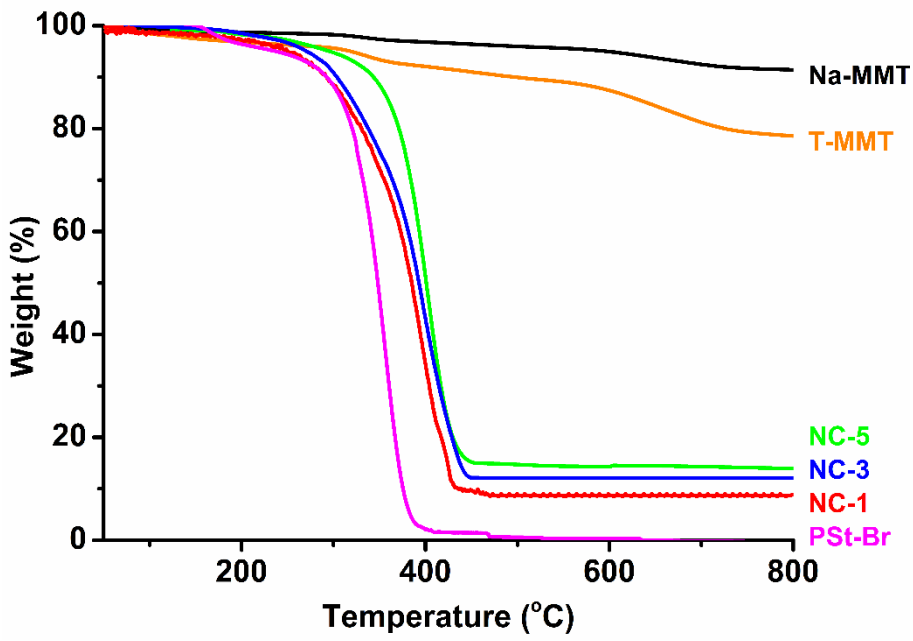

Figure 2.4 : TGA thermograms of Na-MMT, T-MMT, PSt-Br and PSt/MMT nanocomposites.

In summary, the ATRNCchemistry has been extensively used for past years in synthesis of various complex macromolecular architectures.Applied to polymer/clay nanocomposites, this reaction demonstrated its potential and versatility.Spectroscopic and microscopic investigations revealed that successful nanocomposite formation has been achieved by this method. By addition of small amounts of layered silicate loadings resulted in remarkable improvements of thermal properties of nanocomposites. The ATRNC chemistry may be an ideal modular methodology for the introduction of a wide variety of moleculesin to clay layers. By applying this approach, one can easily prepare polymer nanocomposites with desired properties, which enhance their importance in material science.

2.1 Experimental

2.1.1 Materials

Sodium montmorillonite (*Cloisite* Na^+; Na-MMT) was purchased from Southern Clay products with cation exchange capacity (CEC) of 92.6 mequiv/100 g and used as received. Styrene (St, 99 %, Aldrich) was passed through a basic alumina column to remove the inhibitor. *N, N, N', N'', N''*-pentamethyl diethylenetriamine (PMDETA, 99 %, Aldrich) as a ligand, was distilled before use. Ethyl-2-bromopropionate (99 %, Aldrich) and copper(I) chloride (97%, Aldrich) were used as received. Quaternary ammonium-2,2,6,6-tetramethyl-1-piperidinyloxy (Q-

TEMPO) synthesized according to the literature procedure[30]. Other solvents were purified by conventional drying and distillation procedures.

2.1.2 Preparation of organically modified clay (T-MMT)

The organically TEMPO-modified montmorillonite (T-MMT) was prepared through cationic exchange between Na-MMT and quaternary ammonium-2,2,6,6-tetramethyl-1-piperidinyloxy in an aqueous solution. A separate solution of MMT (50 mg) and Q-TEMPO (20 mg, 0,1 mmol) was dispersed in 10 ml of deionized water at 50 ^{o}C for 24 h. Then the two solutions were mixed vigorously and the total volume was brought up to 100 mL and stirred for 24 h at 50 ^{o}C. After mixing, The T-MMT was recovered by filtering the solution, followed by repeated washings of the filter cake with deionized water to remove the excess of ions. The final product was dried in a vacuum oven at room temperature for 24 h.

2.1.3 Preparation of polystyrene by ATRP (PSt-Br)

CuCl (0.25 g, 1.72 mmol), PMDETA (361 μL 1.72 mmol), ethyl-2-bromopropionate as an initiator (225 μL, 1.72 mmol), and styrene (20 mL, 172 mmol) were introduced in a Schlenktube, and the reaction mixture was degassed by three freeze–pump–thaw cycles and left in vacuo. The tube was heated to 90 ^{o}C in an oil bath and stirred for 45 min. Then the mixture was diluted with THF, and passed through an alumina column to remove the complex salts. Precipitation of the polymer was performed in a ten-fold volume of methanol. The solid was then collected after filtration. (Conversion = 12, $M_{n,theo}$= 2520, $M_{n,GPC=}$ 2300, M_w/M_n= 1.12).

2.1.4 Synthesis of polystyrene/MMT nanocomposites (NC-1, NC-3 and NC-5) via ATRNC Chemistry

The organophilic clay (T-MMT, 1, 3 and 5 % of the monomer by weight), bromide-end functional polystyrene (PSt-Br, 230 mg, 0.1 mmol), N,N,N,N",N" pentamethyldiethylene triamine (PMDETA, 60.3 μL, 0.3 mmol) and copper chloride(CuCl, 9.9 mg, 0.1 mmol), toluene (1 mL as solvent) were mixed into a round bottom flask and then and the reaction mixture was degassed by three freeze-pump-thaw cycles and left in vacuum. The mixture was placed in a thermostated oil bath at 120 ^{o}C for 4 h. At the end of the polymerization, the mixture was precipitated into methanol, filtered, dried and weighted.

2.1.5 Characterization

Molecular weights were determined by gel permeation chromatography (GPC) using an instrument consisting of a Viscotek GPCmax Autosampler, a pump, three ViscoGEL GPC columns (G2000HHR, G3000HHR and G4000HHR), and a Viscotek differential refractive index (RI) detector with a THF flow rate of 1.0 mL min–1 at 30°C. The RI detector was calibrated with polystyrene standards having narrow molecular weight distribution. Data were analyzed using Viscotek OmniSEC Omni–01 software. The powder X-ray diffraction (XRD) measurements were performed on a PANalytical X'Pert PRO X-ray diffractometer equipped with graphite-monochromatized Cu Kα radiation (λ = 1.15 Å). Differential scanning calorimetry (DSC) was performed on a Perkin-Elmer Diamond DSC with a heating rate of 20 ºC/min under nitrogen flow (20 mL/min). Thermogravimetric analysis (TGA) was performed on a Perkin-Elmer Diamond TA/TGA with a heating rate of 10 °C/min under nitrogen flow (200 mL/min). Transmission electron microscopy (TEM) imaging of the samples was carried out on a FEI TecnaiTM G2 F30 instrument operating at an acceleration voltage of 200kV. Ultrathin TEM specimens (about 100 nm) were prepared by using a cryo-ultramicrotome (EMUC6 + EMFC6, Leica) equipped with a diamond knife. The ultrathin samples were placed on holey carbon-coated grids for TEM analyses.

3. IN-SITU SYNTHESIS OF A_3-TYPE STAR POLYMER/CLAY NANOCOMPOSITES BY ATOM TRANSFER RADICAL POLYMERIZATION

Through the combination of organic and inorganic compounds in one single material at nanoscopic level is one of the most effective approaches for producing new materials with advanced properties that were usually unavailable in the past[31]. These hybrid materials are easily available due to unique availability of the inorganic nanofillers such as, clays, carbon nanotubes, graphites, polyhedral oligomeric silsesquioxane (POSS) and metal oxides[32]. Among the various nanometric fillers, silicate-based clays are preferred being indeed the best candidates for their superior mechanical, thermal and most important - optical properties[1]. Several synthetic approaches namely, solution exfoliation, melt intercalation, in-situ polymerization, and template synthesis, have been used for the preparation of polymer/clay nanocomposites[2]. The in-situ polymerization is widely used method to prepare polymer/clay nanocomposites because of the types of nanofillers and polymer precursors can be varied in a wide range to get the enhanced properties[33]. In this method monomer, initiator, and/or catalyst are intercalated into silicate layers and the in-situ polymerization is initiated by externally stimulation such as thermal, photochemical, or chemical activation. The growth of polymer chains within the clay galleries not only triggers to the exfoliation of the layered silicate in the polymer matrix but also results the formation of polymer/clay nanocomposites. The main challenge in nanocomposite synthesis is to develop reliable and versatile methods that ensure and maintain the random dispersion of the single silicate layers and, simultaneously, provide more control over the polymer architecture, such as functionality, composition, and dimensions. These well-defined structures also increase the interaction between the polymer matrix and the silicate layers and thereby increase the probability of forming exfoliated nanocomposites. The best way to achieve such a control is by using living and controlled/living polymerization methods[4, 34]. Although most of the efforts have been concentrated on homopolymer-based nanocomposites[5, 6, 9-14, 18-20, 35-38], there is also interest

in nanocomposites containing complexes macromolecular architectures because of their structural and technological significance[39]. However, there are few reports on in situ preparation of nanocomposites containing block[7, 40-44], graft copolymers[45, 46] and hyper-branched polymers[47-50]. Star polymers exhibit different properties from those of their linear counterparts, such as less entanglement in the solid state, high solubility in various solvents, low melt viscosity and fast molecular motion. Previously, Singh et. al used a self-consistent field theory to investigate the interactions between clay layers and star-shaped polymers[51]. It was reported that the relatively compact size of the star polymer combined with the surface of the clay promotes the miscibility of the nanocomposites. Later on, this behavior was proved experimentally by Robello et al. who prepared star polymer/montmorillonite nanocomposites by melt blending technique using star-shaped polystyrene with five arms (M_n = 37100, PDI = 1.25) and organically modified MMT (Cloisite 10A or 15A)[52].

In the present work, we synthesized a quaternary tri-functional atom transfer radical polymerization (ATRP) initiator, which can be directly intercalated into the silicate layers by ion exchange reaction. In situ ATRP of methyl methacrylate (MMA) leads to A_3-type star polymer/MMT nanocomposites possessing partially exfoliated/intercalated nanolayers in the polymer matrix.

3.1 Experimental

3.1.1 Materials

Sodium montmorillonite (Cloisite Na^+; Na-MMT) was purchased from Southern Clay products with cation exchange capacity (CEC) of 92.6 mequiv/100 g used as received. Methyl methacrylate (MMA, 99%, Aldrich) was passed through a basic alumina column to remove the inhibitor. N, N, N', N'', N'' pentamethyldiethylenetriamine (PMDETA, 99 %, Aldrich) as a ligand, was distilled before use. Triethanolamine (98%, Aldrich), triethylamine (99%, Aldrich), 1-bromooctadecane (97%, Aldrich) and copper(I) chloride (97%, Aldrich), 2-bromoisobutyryl bromide (98%, Aldrich) were used as received. Other solvents were purified by conventional drying and distillation procedures.

3.1.2 Synthesis of trifunctional ATRP initiator (Tris-ATRP initiator)

Triethanolamine (5.0 g, 33.5 mmol) and triethylamine (60 ml) were added to 200 ml dry THF. 2-Bromoisobutyryl bromide (24.7 ml, 45.98 g, 0.2 mol) was added drop-wise to this mixture over 1 h at 0 ^{o}C. After stirring for a further 2 h, the triethylammonium hydrochloride salt was removed by filtration and the resulting clear solution was concentrated under vacuum at 30 °C before washing with 0.1 M Na_2CO_3. The product was extracted three times with dichloromethane and the combined organic extract was dried with magnesium sulfate. Removal of the solvent under vacuum afforded a dark-reddish brown oil (18 g, yield: 90 %)[53].

3.1.3 Synthesis of quaternary trifunctional ATRP initiator (Q-tris-ATRP initiator)

The initiator (8.9 g; 15 mmol) solved in 30 ml dry ethanol, 1-bromooctadecane (6.7 ml, 30 mmol) was added and the mixture was stirred 2 days at 70 ^{o}C. After evaporation, the residue was recrystallized in the mixture of acetone and ethanol three times. Then, it was dried in vacuo at ambient temperature for 24 h (9.3 g; yield: 60%). IR (ATR, cm-1): 3650, 3400, 2930, 2850, 1660, 1470, 1400, 1120, 1000, 910, 790, 720, 605.

^{1}H-NMR (D_2O): 1.20–1.35(37H), 1.80–1.90(18H), 2.55–2.65(6H), 3.35–3.45(6H) ppm.

^{13}C-NMR (D_2O): 8.5(-CH_3), 22.3(-CH_2-), 25.9 (-CH_2-), 29.5 (-CH_2-), 33.5 (CH_3-C-Br), 51.5 (CH_3-C-Br), 59.5 (-O-CH_2–CH_2-N), 63.0 (-CH_2–CH_2-N), 64.5 (-O-CH_2–CH_2-N), 171.1 (-C=O) ppm.

3.1.4 Preparation of organically modified clay (O-MMT)

The organically modified montmorillonite (O-MMT) containing trifunctional ATRP initiator was prepared through cationic exchange between sodium montmorillonite (Na-MMT) and Q-tris-ATRP initiator in an aqueous solution. A separate solution of MMT (1 g) and Q-tris-ATRP initiator (0.5 g, 0.6 mmol) was dispersed in 50 mL of deionized water at 50 ^{o}C for 24 h. Then, the two solutions were mixed vigorously and the total volume was brought up to 100 mL and stirred for 48 h at 50 ^{o}C. After

mixing, the T-MMT was recovered by filtering the solution, followed by repeated washings of the filter cake with deionized water to remove the excess of ions. The final product was dried in a vacuum oven at room temperature for 24 h.

3.1.5 Synthesis of A_3-type star polymer/clay nanocomposites

The organophilic clay (O-MMT, 1, 3, 6 and 10 % of the monomer by weight), monomer (MMA, 130 mmol, 1.872 g), ligand (PMDETA, 9.6.10-3 mmol, 2 μL) and copper(I) chloride (CuICl, $9.6.10^{-3}$ mmol, 1.4 mg) and toluene (2 mL as solvent) were mixed into a round bottom flask. The reaction mixture was degassed by three freeze-pump-thaw cycles and left in vacuum. The mixture was placed in a thermostated oil bath at 90 ºC for 16 h. At the end of the polymerization, the mixture was precipitated into methanol, filtered, dried and weighted.

3.1.6 Characterization

Molecular weights were determined by gel permeation chromatography (GPC) using an instrument consisting of a Viscotek GPCmax Autosampler, a pump, three ViscoGEL GPC columns (G2000HHR, G3000HHR and G4000HHR), and a Viscotek differential refractive index (RI) detector with a THF flow rate of 1.0 mL min–1 at 30°C. The RI detector was calibrated with polystyrene standards having narrow molecular weight distribution. Data were analyzed using Viscotek OmniSEC Omni–01 software. Before the GPC measurement, the polymer was cleaved from clay by LiBr refluxing in tetrahydrofuran for about 24 h, followed by centrifugation and filtration through a filter. The powder X-ray diffraction (XRD) measurements were performed on a PANalytical X'Pert PRO X-ray diffractometer equipped with graphite-monochromatized Cu Kα radiation (λ = 1.15 Å). Differential scanning calorimetry (DSC) was performed on a Perkin-Elmer Diamond DSC with a heating rate of 20 ºC/min under nitrogen flow (20 mL/min). Thermogravimetric analysis (TGA) was performed on a Perkin-Elmer Diamond TA/TGA with a heating rate of 10 °C/min under nitrogen flow (200 mL/min). Transmission electron microscopy (TEM) imaging of the samples was carried out on a FEI TecnaiTM G2 F30 instrument operating at an acceleration voltage of 200kV. Ultrathin TEM specimens (about 100 nm) were prepared by using a cryo-ultramicrotome (EMUC6 + EMFC6, Leica) equipped with a diamond knife. The ultrathin samples were placed on holey carbon-coated grids for TEM analyses.

3.2 Results and Discussion

Star polymers are essentially prepared either by the "arm-first" method, where preformed polymer chains are linked to the central core or the "core-first" method, where polymer chains are grown from a multifunctional core initiator. Because of a variety of controlled/living polymerization methods and their accompanying choice of monomers, the core-first method is a versatile and efficient synthetic strategy, and it has been widely used. Our synthetic strategy is based on designing a core molecule possessing both intercalation and multi-functional initiator functionalities to be used for atom transfer radical polymerization (ATRP) of methyl methacrylate. This was done in a two-step procedure; (i) esterification reaction between 2-bromopropionyl bromide and triethanolamine, and (ii) quaternization of trifunctional ATRP initiator with 1-bromooctadecane (Figure 3.1). The characteristic peaks of tri-functional ATRP initiator were determined in ^{1}H-NMR spectrum (Figure 3.2).

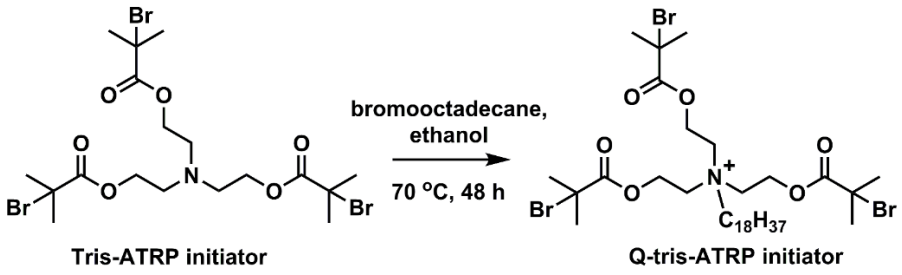

Figure 3.1 : Synthesis of quaternized tri-functional ATRP initiator (Q-tris-ATRP initiator)

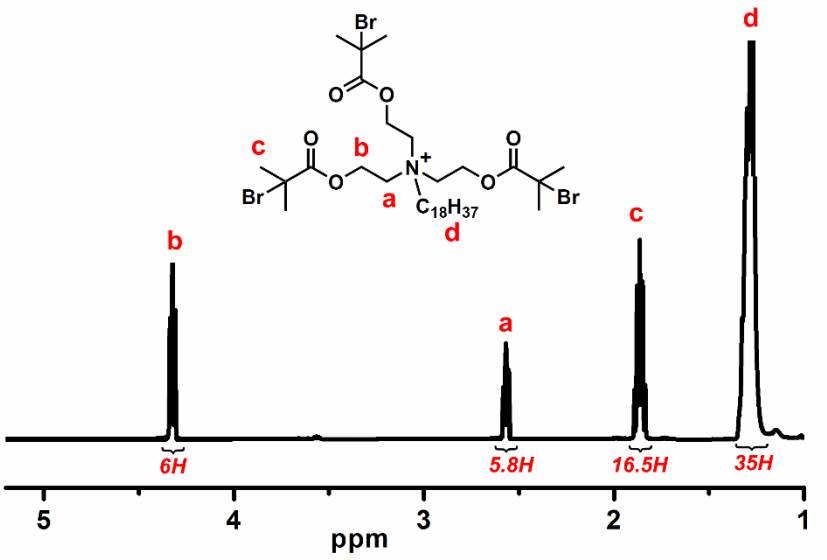

Figure 3.2 : ^{1}H-NMR spectrum of Q-tris-ATRP initiator

The structure of the resulting quaternized tri-functional ATRP initiator (Q-tris-ATRP initiator) was confirmed by spectral analysis.The successful incorporation of Q-tris-ATRP initiator into the clay surface was confirmed by FT-IR, XRD and TGA analyses.The characteristic peaks at 1740 and 1005 cm^{-1} are attributed to C=O and Si-O group of the Q-tris-ATRP initiator and clay in the FT-IR spectrum (Figure 3.3). On the other hand, the diffraction peak was shifted to a lower angle after ion exchange, indicating an increase of the interlayer distance of the clay sheets of 0.4 nm for the organophilic clay (O-MMT). This change indicated that the Q-tris-ATRP initiator was successfully intercalated into the silicate galleries of the MMT clay.

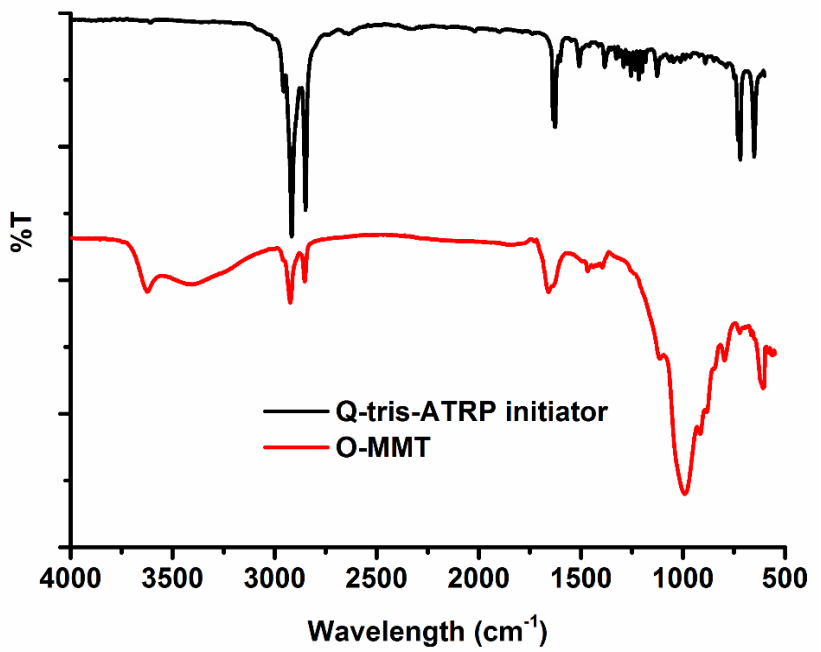

Figure 3.3 : FT-IR spectra of Q-tris-ATRP initiator and organo-modified montmorillonite clay

The thermal gravimetric analysis (TGA) was performed to calculate the organic content of O-MMT after modification. The mass losses were 7.1 % and 20.1% for sodium-montmorillonite (Na-MMT) and O-MMT, respectively corresponding to 13% attachment of Q-tris-ATRP initiator (Figure 3.4).

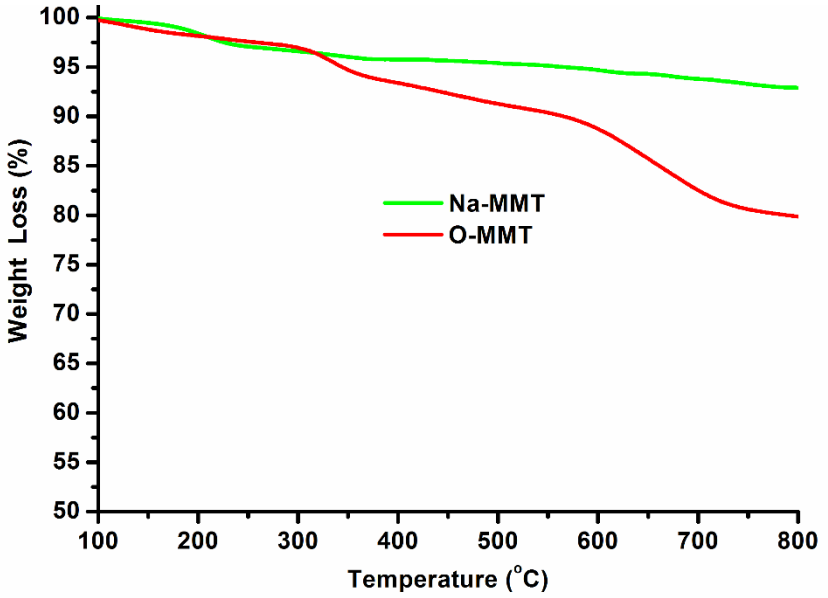

Figure 3.4 : TGA thermograms of sodium and organo-modified montmorillonite clays

ATRP of MMA was carried out at 90 °C in bulk, using O-MMT as multifunctional ATRP initiator and Cu(I)Br as catalyst in combination with PMDETA as ligand. The kinetic plot and the evolution of molecular weight and distribution with conversion for the ATRP targeting DP = 100 were investigated. The monomer consumption ($\ln([M]^0/[M])$) versus the polymerization time plots was linear, which indicated that the propagating radical concentrations were almost constant during the polymerization (Figure 3.5). The molecular weights increased linearly with conversions, which were consistent with the polymerizations proceeding in a controlled fashion. The molecular weight distribution remained narrow (1.45~1.62) and unimodal during the polymerization. However, the experimental molecular weights were much higher than the theoretical values, indicating low initiation efficiency. This might be due to the restricted mobility of Q-tris-ATRP initiator tethered nanoclay platelets.

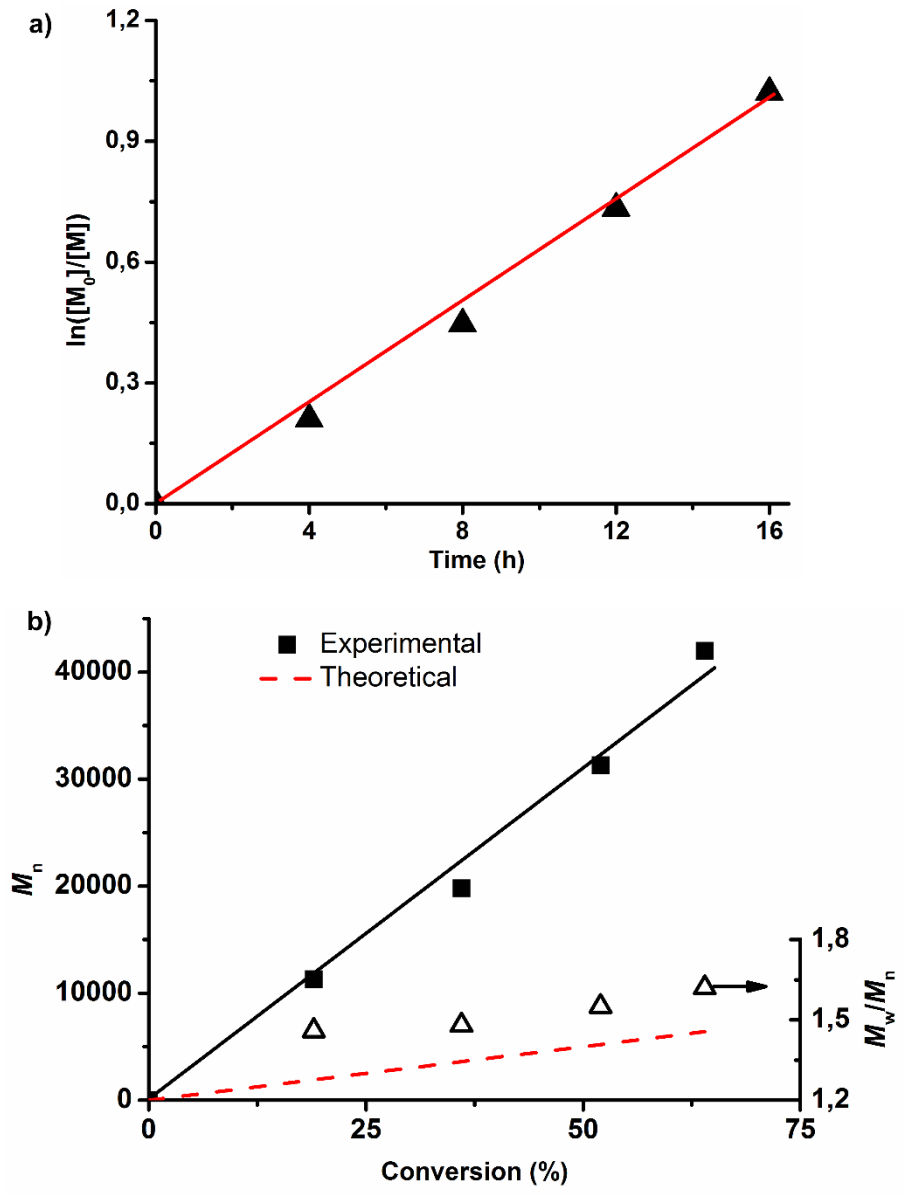

Figure 3.5 : ATRP of methyl methacrylate ($[MMA]_0/[R\text{-}X]_0/[Cu^IBr]_0/[L]_0$ = 100/1/3/3),a) kinetic plot and b) molecular molecular weights and distributions of resulting polymers as a function of degree of conversion.

Table 3.1 summarizes the results of ATRP of MMA in the presence of different amount of nanoclay. The polymer obtained in the absence of nanoclay (Table 3.1, NC-0) had molecular weight value close to the theoretical one and relatively narrow molecular weight distribution (1.48). Compared to the heterogeneous system, it showed better control of molecular weight and distribution under the same experimental conditions. With an increase in nanoclay initiator amount, there was an increase in polymerization rate, which results in the higher conversion of MMA polymerization and lower the molecular weights of the resulting polymers.

Table 3.1 : ATRP of methyl methacrylate in the presence of different amount organophilic clay.

Run[a]	O-MMT (wt%)	[MMA]/[R-X]/[L]/ [$Cu^{I}Br$]	Cnv[b] (%)	$M_{n,GPC}$[d] [g.mol^{-1}]	$M_{n,GPC}$[d] [g.mol^{-1}]	Mw/M_n[d]
NC-0	0	100/1/3/3	78	7,900	17,000	1.48
NC-1	1	100/1/3/3	62	6,400	42,000	1.62
NC-3	3	50/1/3/3	77	4,200	28,000	1.67
NC-6	6	50/1/3/3	86	4,100	23,000	1.45
NC-10	10	30/1/3/3	91	3,000	19,000	1.53

[a] Polymerization reaction was carried out in bulk at 90 °C for 16 h. [b] Determined by gravimetrically. [c] $M_{n,Th}$= $[MMA]_0/([R\text{-}X]_0$ x $M_{w,MMA}$x Cnv. [d] Molecular weight and distribution were determined by gel permeation chromatography

XRD diffractograms of Na-MMT (6.95°), O-MMT (6.82°) and PMMA/MMT nanocomposites at different clay loading are illustrated in Fig. 3.6. The basal space (d_{001}) was expanded after the cation exchange with Q-tris-ATRP initiator from 1.28 nm to 1.31 nm. After the polymerization, this peak disappeared in the X-ray diffraction pattern of NC-1 sample, which indicates the formation of exfoliated structure of clay. However, it was found that partially exfoliated or intercalated structures existed in the high clay content system (NC-3, 6 and 10) probably due to the difficulty for overcoming the intensive ionic attraction between the neighboring platelets.

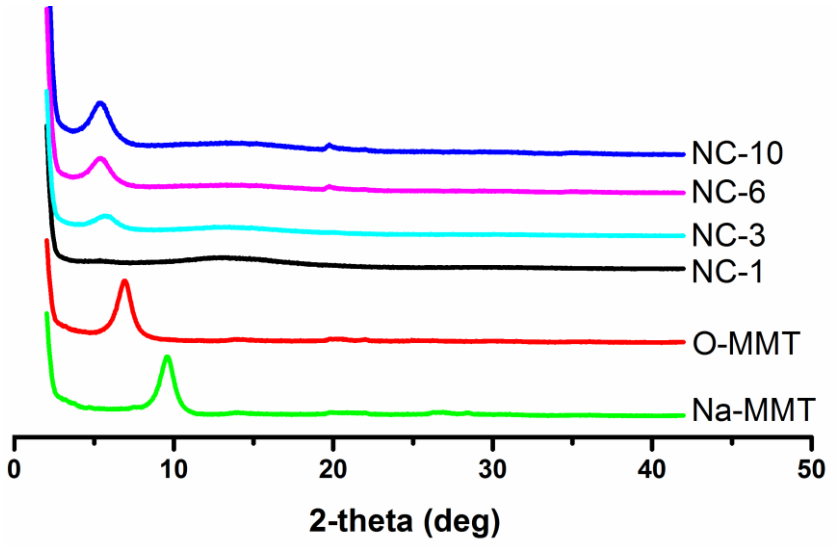

Figure 3.6 : X-ray diffractions of Na-MMT, O-MMT and obtained nanocomposites (NC-1, 3, 6 and 10).

Although XRD is a convenient and practical tool to determine intercalated and exfoliated morphologies, in certain cases its reliability is limited due to the clay dilution, preferred orientation, mixed layering and other peak broadening factors. Direct imaging techniques such as atomic force microscopy (AFM), scanning electron microscopy (SEM) or transmission electron microscopy (TEM) are often combined to strengthen the conclusion derived from XRD analysis. Fig. 3.7 presents the high magnification transmission electron microscope images of the nanocomposites containing 1, 3, 6 and 10 wt % O-MMT, respectively. The dark lines represent the silicate layers; about 1.0 nm thick and from 50 to 100 nm in lateral dimension, which are oriented perpendicularly to the slicing plane and the gray areas correspond to the polymer matrix. As the TEM images showed that the dispersion of clay exhibits different morphologies, including intercalated regions with a non-uniform separation of the layers and exfoliated single layers isolated from any stack. TEM analysis also confirmed that the degree of exfoliation in the nanocomposites decreased with increasing clay loading in the process. This might be due to the high loading degree or molecular weight of polymer matrix. The polymer with higher molecular weight (NC-1) is more beneficial for exfoliated structure than low molecular weight polymer (NC-3, 6 and 10). Combined together with the results of XRD and TEM, it could be concluded that the interlayer spacing derived from XRD is just an average value for a mixed morphology of intercalated and exfoliated clays, and not an actual value for a well-defined interlayer distance in regularly intercalated montmorillonites.

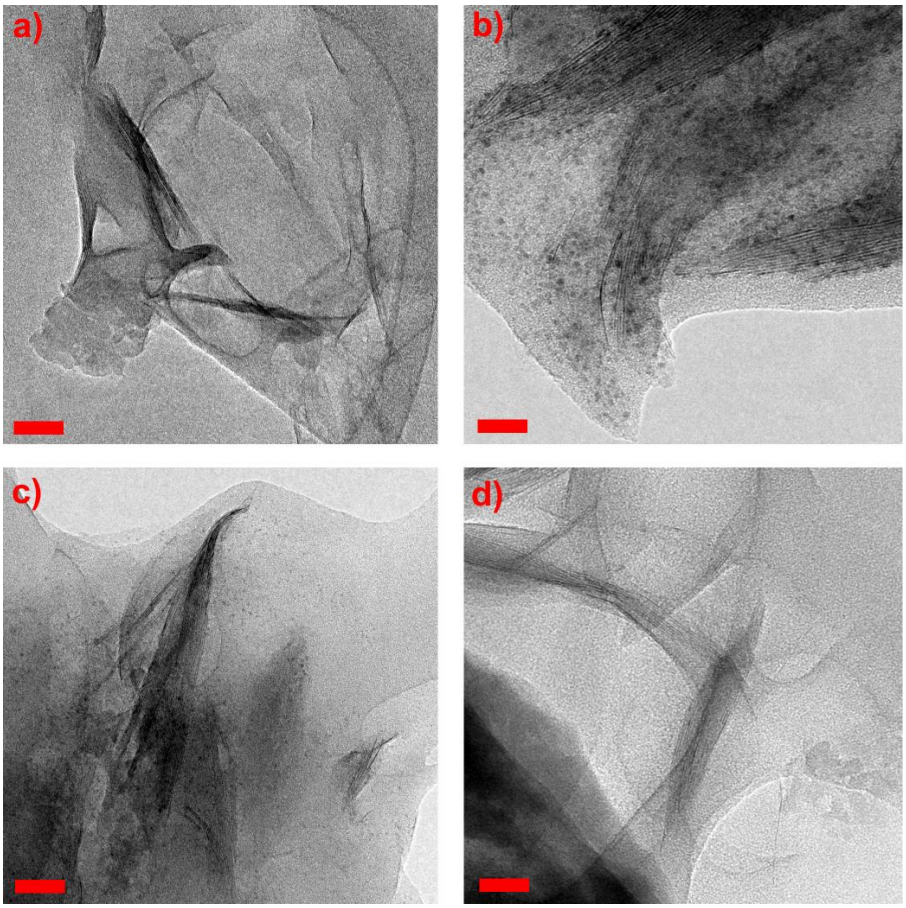

Figure 3.7 : TEM micrographs showing exfoliated/intercalated silicate layers in NC-1 (a), NC-3 (b), NC-6 (c) and NC-10 (d) samples at higher magnification (scale bar: 20 nm).

Thermal degradation behavior of neat A_3-PMMA star polymer and PMMA/MMT nanocomposites at various loading prepared via ATRP was studied by TGA, heating from room temperature to 800^{o}C under inert atmosphere. As indicated in Fig. 3.8, the thermal behavior of the nanocomposite is quite similar to the neat polymer and single step decomposition was observed for all nanocomposite samples. It was found that the nanocomposites had much higher T_{onset} (temperature at 5% weight loss) and T_{max} (temperature at 50% weight loss) than the neat polymer (Table 3.2). This beneficial effect can be explained by addition of clay as an inorganic material with high thermal stability and great barrier properties that can prevent the heat from transmitting quickly and can limit the continuous decomposition. However, the thermal degradation temperatures of the nanocomposites with different organic clay loadings were very close to each other, and no significant trend with increasing clay content was observed. Notably, the final char yields of nanocomposites were increased with increase in weight percent of clay loading.

Table 3.2 : Physical properties of PMMA/MMT nanocomposites and their components for comparison.

Entry	d_{001}[a] (nm)	T_g[b] (°C)	Weight loss Temperature[c] (°C)		Char Yield[c] (%)
			%10	%50	
Na-MMT	0.90	-	-	-	92.9
O-MMT	1.30	-	565	-	79.9
A_3-PMMA	-	123.1	286	348	<1
NC-1	-	130.8	300	361	2.3
NC-3	1.55	128.4	313	369	4.1
NC-6	1.60	128.3	316	374	6.4
NC-10	1.66	129.0	325	382	10.9

[a] Basal spacing (d_{001}) is calculated by XRD analysis. [b] Determined by DSC and analyses under a nitrogen flow at a heating rate of 10 °C/min. [c] Determined by TGA analysis under a nitrogen flow at a heating rate of 10 °C/min.

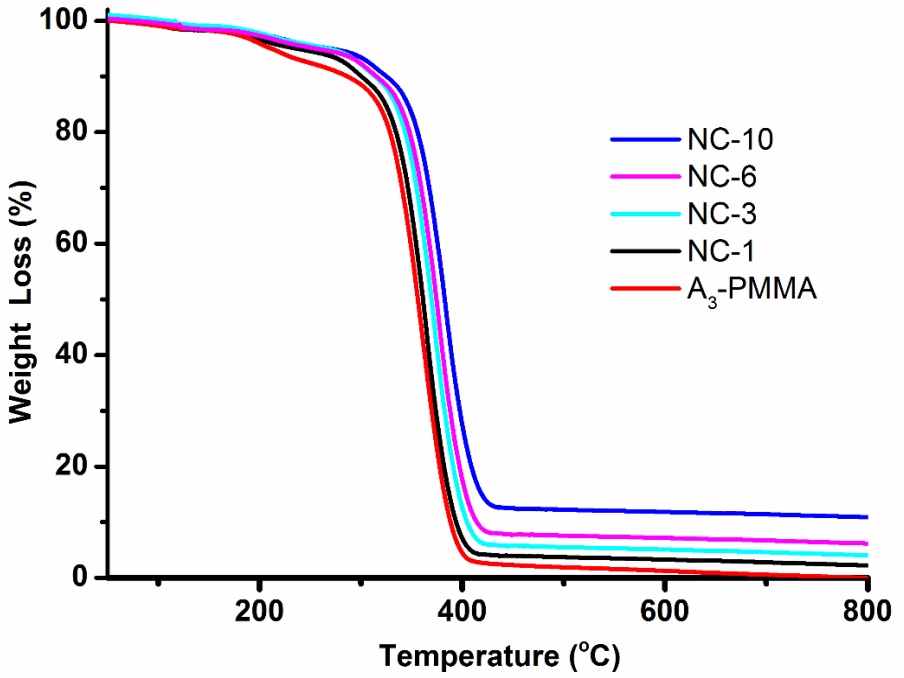

Figure 3.8 : TGA thermograms of A_3-PMMA and PMMA/MMT nanocomposites (NC-1, 3, 6 and 10).

Differential scanning calorimetry (DSC) analysis of neat A_3-PMMA star polymer and PMMA/MMT nanocomposites was carried out to determine glass transition temperature (T_g) values of the nanocomposites at various clay loadings (Fig. 3.9). The Tg of polymers depends mainly on the molecular structure of the polymer (chain stiffness, number, architecture and bulkiness of the side groups, and the inter- and

intra-molecular interactions) and on the crosslink density of the polymer. All nanocomposite samples had high Tg value than neat polymer. The highest value of NC-1 nanocomposite can be ascribed to its molecular weight and exfoliation morphology with fine dispersion of silicate layers in the polymer matrix that provides large surface area for clay interacting with polymer matrix, which can be lead to the restricted segmental motions near the organic-inorganic interfaces. Conclusively, there was no significant improvement of T_g of nanocomposites with the increase of the clay content.

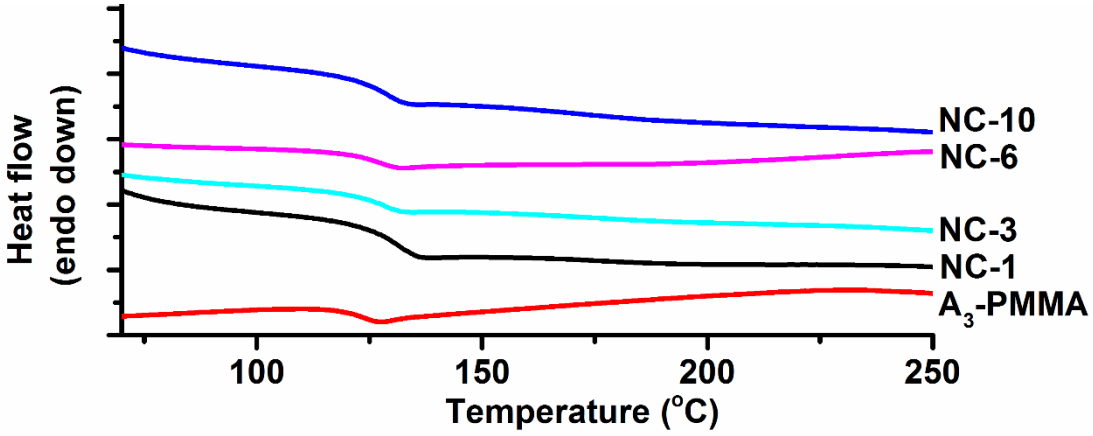

Figure 3.9 : DSC traces of A_3-PMMA star polymer and PMMA/MMT nanocomposites (NC-1, 3, 6 and 10).

3.3 Conclusions

The sodium montmorillonite was successfully functionalized with tri-functional ATRP initiator, which was confirmed by XRD, TGA and FT-IR analyses. A series of A_3-PMMA star PMMA/MMT nanocomposites have been prepared by in-situ ATRP of MMA. Linear kinetic plot and increase in molecular weight with conversion indicated that ATRP of MMA was controlled. Spectroscopic and microscopic investigations revealed a complex morphology, with partial intercalation/exfoliation, which depends on the concentration of clay. DSC and TGA analyses showed that all nanocomposites have higher T_g value and thermal stabilities compared to neat A_3-PMMA star polymer.

The exfoliated nanocomposite has been obtained when polymerization was conducted with 1% of organic clay loading. However, with increasing the clay loading to 3, 6 and 10%, the degree of exfoliation of the nanocomposites decreased, which confirmed by both XRD and TEM analyses. This may be due to short chain

length of branches of the star polymer. From TGA, an improvement in the thermal stability of obtained nanocomposites was noted even at 1% of clay loading.

4. POLYMER/CLAY NANOCOMPOSITES THROUGH MULTIPLE HYDROGEN-BONDING INTERACTIONS

Over the last two decades, various types of nanofillers have been used for the preparation of nanocomposites with almost all types of polymer matrices[2]. However, polymer nanocomposites based on clays attract great interest in today's materials research because they are naturally abundant, economical, and more important, benign to the environment[3]. But the dispersion of this kind of nanofillers is not straightforward. In most cases, surface modification of these materials is required to obtain organically modified silicates or clay which then is more compatible with the organic polymer matrices. Generally, the addition of small amount of clay into polymer-based materials resulted in an impressive property enhancements, such as high moduli, increased strength and heat resistance, decreased gas permeability and flammability[54].

Up to date, a number of synthesis routes have been developed to fabricate polymer nanocomposites with homogenous dispersion of clay layers, in solution mixing, melt mixing and *in-situ* polymerization[55]. Due to the direct synthesis via polymerization along with the presence of organoclays, the *in-situ* polymerization is most widely used technique to produce polymer nanocomposites with homogeneous distribution of the clay layers inside the polymer matrix[4, 33]. In this route, organoclay containing monomer, initiator or catalyst functionalities is first dispersed in the monomer or monomer solution, and then the resulting mixture is polymerized by standard polymerization methods. The in-situ polymerization can be initiated by externally stimulation such as thermal[7, 10, 56, 57], photochemical[6, 9, 11, 12, 39, 58-62] or chemical activation. The growth of polymer chains within the clay galleries may lead to the clay exfoliation and hence the nanocomposite formation[13, 14, 36, 63]. Recently, a conceptually different approach, namely copper (I) catalyzed azide/alkyne cycloaddition (CuAAC) "click" reaction, in which exfoliation is rooted in the functional units of the intercalant that readily react with the antagonist groups of the preformed polymers[18-20, 35]. In this approach, azide and alkyne partners could each be incorporated in either the clay surface or polymer chain. The

quantitative efficiency of coupling reaction coupled with tolerance to a wide variety of functional groups and reaction conditions make this coupling process highly attractive for the nanocomposite preparation.

Molecular self-assembly is a powerful method for the construction of well-defined nanoarchitectures and for the tailoring of physical properties of small molecular building blocks[64, 65]. With this method, a variety of nanostructures including micelles, vesicles, liquid crystal phases, and Langmuir monolayers by surfactant molecules and supramolecular assemblies can be constructed by means of non-covalent interactions, such as hydrogen bonding, metal coordination, hydrophobic forces, van der Waals forces, π-π stacking, and/or electrostatic interactions. Among them, hydrogen bonding system is the most crucial and favorite secondary interaction to construct supramolecular architectures due to their moderate strength, high directionality and selectivity. However, the hydrogen bond pairs are weak relative to covalent and ionic bonds, and therefore, the application of synthetic hydrogen bonding systems require the use of multiple hydrogen-bonding interactions. In this regard, 2-ureido-4[^{1}H]pyrimidinone (UPy) functionality is a promising unit which can undergo very strong and highly directional self-complimentary quadruple hydrogen bonding through their dimerization[66]. The UPy-based hydrogen-bonding system has been applied for the preparation of supromolecular polymers[67, 68] from the corresponding telechelics prepared with a variety of polymer backbones including poly(ethylene oxide)s[69], poly(butadiene)s[70], poly(dimethyl siloxane)s[71], poly(styrene)s[72] and poly(methyl methacrylate)s[72, 73]. However, this chemistry has been scarcely applied for the preparation of supramolecular polymer nanocomposites using graphenes, carbon nanotubes, and gold hydroxyapatite and silica nanoparticles as nanofiller. To the best of our knowledge, no report is currently available in open literature regarding the use of UPy-based hydrogen-bonding system in the preparation of polymer/clay nanocomposites.

In the present work, we synthesized an UPy-functionalized organoclay from commercial montmorillonite clay (Closite 30B) containing two hydroxyl groups by urethane formation with UPy-isocyanate. The UPy-end functionalized poly(ethylene glycol) and poly(ε-caprolactone) were chosen as matrix polymer for nanocomposites due to their synthetic accessibilities and existing knowledge on their

characterizations. The multiple hydrogen-bonding interactions of the intercalated UPy-functionalized organoclay and UPy-end functionalized polymers could gradually push the layers apart, leading to delamination of clay tactoids and lead to formation of nanocomposites. The synthetic capabilities of this approach can be greatly extended by careful choices of organoclays and polymers, and the optimization of supramolecular interactions as well.

4.1 Experimental

4.1.1 Materials

Organo-modified clay, Cloisite 30B [MMT-$(CH_2CH_2OH)_2$] was purchased from Southern Clay Products (Gonzales, TX, USA) The organic content of the organo-modified MMT, determined by Thermo Gravimetric Analysis (TGA), was 21 wt %. Before use, the clay was dried under vacuum at 110 ^oC for 1 h.Tin(II) 2-ethyl-hexanoate ($Sn(Oct)_2$, Aldrich, 95 %), poly(ethylene glycol) methyl ether (Me-PEG, Aldrich, M_w= 2000 g/mol), 2-amino-4-hydroxy-6-methylpyrimidine (Aldrich, 98 %), hexamethylene diisocyanate (HMDI, Aldrich, 99%≤), dibutyltin dilaurate (Aldrich, 95 %), 1-butanol (Merck, 99.5 %), pyridine (Merck, 98 %), ethanol (Merck, 96 %), pentane (Merck, 98 %), acetone (Merck, ACS), toluene (Merck, 99 %) and hydrochloric acid (HCl, Merck, 32 %) were used as received. Epsilon-caprolactone (CL, Aldrich, 97 %) was vacuum distilled over calcium hydride.

4.1.2 Synthesis of 2-(6-isocyanatohexylamino carbonylamino)-6-methyl 4[1H] pyrimidinone (UPy-isocyanate)

UPy-isocyanate was prepared according to the modifed literature procedure[74]. 2-Amino-4-hydroxy-6-methyl pyrimidine (8.6 g, 70 mmol) was added to a 250 mL round bottomed flask. 1,6-Hexamethylene diisocyanate (HMDI, 76 mL, 475 mmol) and pyridine (5 mL) were then added, the flask fitted with a reflux condenser, and the mixture stirred at 100 ^oC overnight under dry nitrogen. Pentane (30 mL) was then added and the solid product, a white powder, collected by filtration. The solid product was washed 3 times with 125 mL portions of acetone to remove unreacted HMDI and then dried overnight under high vacuum at 50 ^oC (18.5 g; yield: 90%).

^{1}H-NMR ($CDCl_3$): δ = 13.14 (s, 1H, CH_3–C–N<u>H</u>), 11.87 (s, 1H, CH_2–NH–(C=O)–N<u>H</u>), 10.19 (t, 1H, CH_2–N<u>H</u>–(C=O)–NH), 5.82 (s, 1H, C<u>H</u>=C–CH_3), 3.27 (m, 4H,

NH–(C=O)–NH–C$\underline{H}_2$+C$\underline{H}_2$–NCO), 2.23 (s, 3H, C$\underline{H}_3$), 1.61 (m, 4H, N–CH_2–C$\underline{H}_2$), 1.41 (m, 4H, CH_2–CH_2–C$\underline{H}_2$–C$\underline{H}_2$–CH_2–CH_2–NCO) ppm.

FT-IR (ATR): υ = 3320, 2930, 2260 (NCO stretch), 1700 (UPy), 1670 (UPy), 1620 (urea), 1580 (UPy), 1520 (UPy), 1460, 1355, 1310, 1255 cm^{-1}.

4.1.3 Synthesis of UPy-end functionalized poly(ethylene glycol) (PEG-UPy)

Me-PEG (2000 mg, 1 mmol) was first dried under vacuum at 90 °C and then dissolved in dry $CHCl_3$. The UPy−isocyanate (880 mg, 3 mmol) and 3 drops of dibutyltin dilaurate (DBDTL) were added the reaction mixture, which was stirred at 60 °C for 16 h. The crude product was precipitated in cold methanol, filtered and dried under vacuum (1.3 g; yield: 65%).

$_1$H-NMR ($CDCl_3$): δ = 13.12 (s, 1H, C–NH–C=N, UPy), 11.84 (s, 1H, CH_2NH–(C=O)–NH, UPy), 10.11 (s, 1H, CH_2NH–(C=O)–NH, UPy), 5.83 (s, 1H, C=CH, UPy), 4.92 (s, 1H, CH_2NH–(C=O)–OCH_2), 4.18 (t, 2H, NH–(C=O)–OCH_2CH_2), 3.74 (t, 2H, NH–(C=O)–OCH_2CH_2), 3.64 (t, 4nH, OCH_2CH_2O), 3.35 (s, 3H, OCH_3), 3.24 (m, 2H, CH_2NH–(C=O)–NH), 3.16 (m, 2H, CH_2NH–(C=O)–OCH_2), 2.23 (s, 3H, CH_3, UPy), 1.59-1.35 (3m, 8H) ppm.

FT-IR (ATR): υ = 3320, 2875, 1700 (UPy), 1670 (UPy), 1620 (urea), 1580 (UPy), 1530 (UPy), 1470, 1420, 1400, 1370, 1290, 1240, 1185 (C–O stretch), 1110, 1040, 940, 840, 810, 770, 740 cm-1.

4.1.4 Synthesis of monohydroxytelechelic poly(ε-caprolactone)

The monohydroxy-telechelic poly(ε-caprolactone) (PCL) of the assumed molar mass (i.e., Mn controlled by the consumed monomer to transfer agent concentrations ratio) was prepared by the CL polymerization initiated with $Sn(Oct)_2$ and 1-butanol (BuOH) as an initiator[75]. Typically, 1-butanol (23.8 μl, 0.26 mmol) and CL (3.2 ml, 30 mmol) were charged in a 50-mL Schlenk flask with a magnetic stirring bar, and a solution of $Sn(Oct)_2$ (8 μl, 0.024 mmol) in 2 mL of toluene was added using a syringe. The reactive mixture was degassed via three pump-freeze-thaw cycles and then immersed in a thermostated oil bath at 120 °C for 4 h. The resulting PCL, after deactivation of the growing species with 2 N HCl(aq) was washed with distilled water (up to neutral pH) and lyophilized under reduced pressure (2.24 g; yield: 70%, $M_{n,GPC}$ = 7650, M_w/M_n = 1.32).

^{1}H-NMR ($CDCl_3$): δ = 4.18 (t, 2H, CH_2–(C=O)–$OCH_2CH_2CH_2CH_3$), 4.06 (t, 2nH, CH_2–(C=O)–OCH_2), 3.65 (t, 2H, HO–$CH_2CH_2CH_2CH_2CH_2$–(C=O)), 2.31 (m, 2nH, CH_2–(C=O)–OCH_2), 1.64 (m, 4nH, CH_2–(C=O)–$OCH_2CH_2CH_2CH_2CH_2$), 1.58 (m, 4H, CH_2–(C=O)–$OCH_2CH_2CH_2CH_3$), 1.39 (m, 2nH, CH_2–(C=O)–$OCH_2CH_2CH_2CH_2CH_2$), 0.96 (t, 3H, CH_2–(C=O)–$OCH_2CH_2CH_2CH_3$) ppm.

FT-IR (ATR): υ = 2940, 2865, 1720 (C=O stretch), 1470, 1420, 1400, 1370, 1290, 1240, 1185 (C–O stretch), 1110, 1065, 1045, 1015, 995, 965, 940, 879, 880, 800, 785, 770, 740 cm-1.

4.1.5 Synthesis of UPy-end functionalized poly(ε-caprolactone) (PCL-UPy)

Synthesis of UPy-PCL carried out according to the following precedure[74]: After addition of poly(ε-caprolactone) (1530 mg 0,2 mmol Mn= 7650 dried 2 hours under vacuum at room temperature), UPy-isocyanate (0,176 mg, 0,6 mmol) in 50 mL round bottom flask were dissolved in 30 mL chloroform and dibutyltindilaurate (10 drops DBTL as catalysis) was added. The resulting solution stirred over night at 60 ^oC and filtered to remove the urea product and precipitated in cold hexane and dried overnight under high vacuum (1.3 g; yield: 85%).

^{1}H-NMR ($CDCl_3$): δ = 13.13 (s, 1H, C–NH–C=N, UPy), 11.76 (s, 1H, CH_2NH–(C=O)–NH, UPy), 10.14 (s, 1H, CH_2NH–(C=O)–NH, UPy), 5.85 (s, 1H, C=CH, UPy), 4.90 (s, 1H, CH_2NH–(C=O)–OCH_2), 4.18 (t, 2H, CH_2–(C=O)–$OCH_2CH_2CH_2CH_3$), 4.06 (t, 2nH, CH_2–(C=O)–OCH_2), 3.24 (m, 2H, CH_2NH–(C=O)–NH), 3.16 (m, 2H, CH_2NH–(C=O)–OCH_2), 2.31 (m, 2nH, CH_2–(C=O)–OCH2), 2.23 (s, 3H, CH_3, UPy), 1.64 (m, 4nH, CH_2–(C=O)–$OCH_2CH_2CH_2CH_2CH_2$), 1.58 (m, 4H, CH_2–(C=O)–$OCH_2CH_2CH_2CH_3$), 1.50 (m, 8H, NH–(C=O)–NH–$CH_2CH_2CH_2CH_2CH_2CH_2$–NH–(C=O)–O), 1.39 (m, 2nH, CH_2–(C=O)–$OCH_2CH_2CH_2CH_2CH_2$), 0.96 (t, 3H, CH_2–(C=O)–$OCH_2CH_2CH_2CH_3$) ppm.

FT-IR (ATR): υ = 3320 (N-H), 2940, 2865, 1720 (C=O stretch), 1700 (UPy), 1670 (UPy), 1620 (urea), 1580 (UPy), 1530 (UPy), 1470, 1420, 1400, 1370, 1290, 1240, 1185 (C–O stretch), 1110, 1065, 1045, 1015, 995, 965, 940, 879, 880, 800, 785, 770, 740 cm-1.

4.1.6 Modification of MMT-$(CH_2CH_2OH)_2$ with UPy-isocyanate (UPy-MMT)

Quaternary ammonium salt modified natural montmorillonite (MMT$(CH_2CH_2OH)_2$, 1 g, 1.22 mmol, OH content) was added in round bottom flask and dried under vacuum at 90 ^oC for 30 min and then UPy-isocyanate (0.64 mg, 2.44 mmol) and chloroform (50 mL) were added[76]. This mixture was flushed with nitrogen for 30 min in chloroform (30 mL), and it was heated to 60 ^oC for 18 h with continuous stirring. The organomodified clays were then collected by filtration with a cold silica filter, washed with chloroform to remove any unreacted UPy-isocyanate, and finally dried in vacuum (1.28 g; yield: 78%).

FT-IR (ATR): υ = 3640 (O-H), 2940 (C-H), 2865 (C-H), 1700 (UPy), 1670 (UPy), 1620 (urea), 1580 (UPy), 1530 (UPy), 1325, 1250, 1240, 1185 (C–O stretch), 1020 (Si-O) cm-1.

4.1.7 Preparation of polymer/MMT nanocomposites by UPy-based hydrogen-bonding system

The organomodified clay (MMT-UPy, 3, 5, 10 and 20 % of the polymer by weight) and polymer (0.07 mmol of PEG-UPy or PCL-UPy) and chloroform (20 mL as solvent) were mixed into a round bottom flask. The reaction mixture was degassed by three freeze-pump-thaw cycles and left in vacuum. The mixture was placed in a thermostated oil bath at 50 ^oC for 16 h. At the end of hydrogen bonding reaction, the mixture was precipitated into diethylether, filtered, dried and weighted.

4.1.8 Characterization

Molecular weights were determined by gel permeation chromatography (GPC) using an instrument consisting of a Viscotek GPCmax Autosampler, a pump, three ViscoGEL GPC columns (G2000HHR, G3000HHR and G4000HHR), and a Viscotek differential refractive index (RI) detector with a THF flow rate of 1.0 mL min–1 at 30°C. The RI detector was calibrated with polystyrene standards having narrow molecular weight distribution. Data were analyzed using Viscotek OmniSEC Omni–01 software. The powder X-ray diffraction (XRD) measurements were performed on a Panalytical X'Pert PRO X-ray diffractometer equipped with graphite-monochromatized Cu Kα radiation (λ = 1.15 Å). Differential scanning calorimetry (DSC) was performed on a Perkin-Elmer Diamond DSC with a heating

rate of 20 ºC/min under nitrogen flow (20 mL/min). Thermogravimetric analysis (TGA) was performed on a Perkin-Elmer Diamond TA/TGA with a heating rate of 10 °C/min under nitrogen flow (200 mL/min). Transmission electron microscopy (TEM) imaging of the samples was carried out on a FEI TecnaiTM G2 F30 instrument operating at an acceleration voltage of 200kV. Ultrathin TEM specimens (about 100 nm) were prepared by using a cryo-ultramicrotome (EMUC6 + EMFC6, Leica) equipped with a diamond knife. The ultrathin samples were placed on holey carbon-coated grids for TEM analyses.

4.2 Results and Discussion

4.2.1 Synthesis and characterization of UPy-end functionalized polymers

After discovery of UPy-based supramolecular polymers, an isocyanate-functionalized UPy (UPy-NCO) synthon was developed for end-functionalization of any hydroxyl or amine-terminated polymers, forming urethane and urea linkages[77, 78]. The UPy-NCO compound was prepared by reacting 2-amino-4-hydroxyl-6-methyl pyrimidine and 1, 6- hexamethylene diisocyanate. On the other hand, monohydroxytelechelic poly(ε-caprolactone) was prepared via ring-opening polymerization of epsilon caprolactone initiated with $Sn(Oct)_2$ and 1-butanol. Whereas, commercially available poly(ethylene glycol) methyl ether has been used directly as received. The next step, UPy-poly(ethylene glycol) (UPy-PEG) and poly(ε-caprolactone) (UPy-PCL) have been prepared from UPy-NCO synthon with corresponding monohydroxytelechelics polymers via urethane formation at 60 ºC for 16h (Figure 4.1).

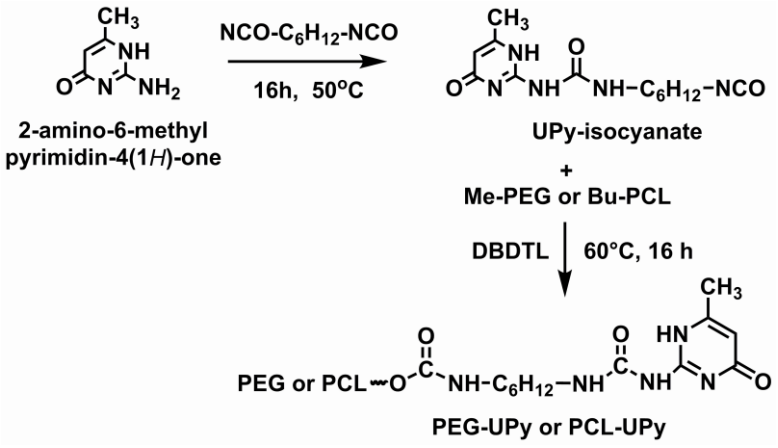

Figure 4.1 : Synthesis of UPy-PEG and UPy-PCL monotelechelics.

The end-group transformations of monohydroxyl end functionalized polymers into UPy group were followed by ^{1}H-NMR and FT-IR techniques. The ^{1}H NMR of the products showed all the characteristic signals corresponding to UPy-PEG and UPy-PCL. The transformation of –NCO group can be also seen from the FT-IR spectra, the C=O stretching peaks at 1670 and 1580 cm^{-1} were observed after the reaction, which indicates the successful attachment of pyrimidinone groups to the polymers.

4.2.2 Functionalization of organomodified nanoclay with UPy-isocyanate.

For the incorporation of UPy units into clay layers, UPy-NCO synthon was used to react with commercial montmorillonite clay containing two hydroxyl groups Cloisite 30B (MMT-$(CH_2CH_2OH)_2$) in chloroform (Figure 4.2).

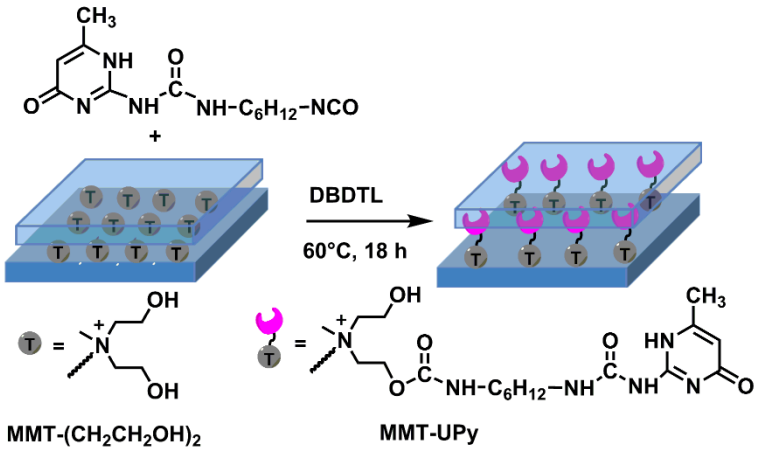

Figure 4.2 : Functionalization of MMT-$(CH_2CH_2OH)_2$ with UPy-isocyanate.

The successful incorporation of UPy groups into the clay surface was confirmed by FT-IR and XRD analyses. The FT-IR spectrum of resulting UPy-MMT showed that a characteristic isocyanate absorbance peak at 2275 cm^{-1} disappeared completely after reaction of UPy-NCO with hydroxyl groups of MMT-$(CH_2CH_2OH)_2$ while the other peaks associated with UPy were still present. In addition, a broad peak at around 3400 cm^{-1} indicates that small amount of non-functionalized hydroxy groups on the surface of the layers was still remained. On the other hand, the XRD diffraction peak was shifted to a lower angle (from 4.89^{o} to 4.75^{o}) after modification, indicating an increase of the interlayer distance of the clay sheets of 0.5 nm for the UPy-MMT. The degree of UPy surface functionality was determined by thermal gravimetric analysis (TGA), which was performed to calculate the organic content of organomodified clays. The mass losses were determined as 20.3 % and 42.7% MMT-

$(CH_2CH_2OH)_2$ and UPy-MMT, respectively.This change indicated that the UPy-NCO synthonwas successfully intercalated into the silicate galleries of the MMT clay (Table 4.1).

4.2.3 Preparation of polymer/MMT nanocomposites by UPy-based hydrogen-bonding system

Strong attractive interactions between the surface of an organoclay and a polymer matrix must exist in order to achieve a high degree of dispersion in organoclay nanocomposites. Among the intermolecular forces including (i) ionic interactions, (ii) ion-dipole interactions, (iii) hydrogen bonding, (iv) dipole-dipole interactions and (v) van der Waals interactions, the hydrogen bonding is typically much stronger than Van der Waals interactions but weaker than ionic interactions. The strength of a hydrogen bonding motif is determined by the number of individual hydrogen bonds involved. To achieve a good macromolecular association, a higher hydrogen bonding association constant K is needed. One of the best-known examples is the multiple hydrogen bonding motif based on UPy group that dimerizes with a strong self-association constant ($K_{dim} > 10^7$ M^{-1} in chloroform) using a self-complementary DDAA (donor–donor–acceptor–acceptor). Another key feature of UPy motif over other hydrogen bonding groups is related to its easy chemistry; it can be attached to many different building blocks. By choosing suitable building blocks, many thermally reversible polymers have been prepared.

In order to take advantage of multiple hydrogen-bonding interactions based UPy chemistry, a series of nanocomposites were prepared by solution blending of the MMT-UPy (MMT-UPy, 3, 5, 10 and 20 % of the polymer by weight) with either PEG-UPy or PCL-UPy in chloroform (Figure 4.3).

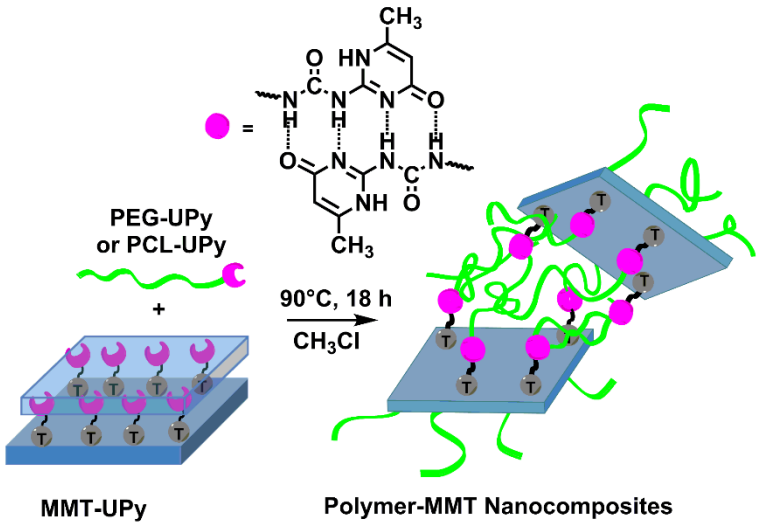

Figure 4.3 : Preparation of PEG/MMT and PCL/MMT nanocomposites.

The infrared absorption spectra of PEG/MMT-20, PCL/MMT-20 nanocomposites and their components were recorded in the region from 600–4000 cm^{-1}, as shown in Figures4.4 and 4.5.

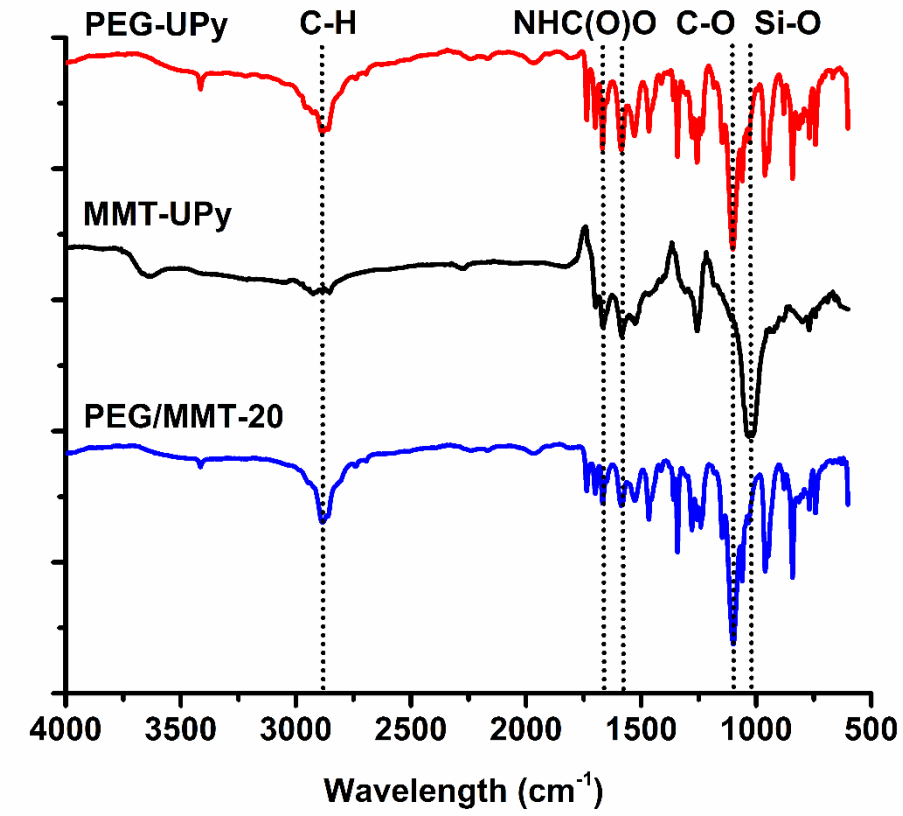

Figure 4.4 : FT-IR spectra ofneat PEG-UPy, MMT-UPy and PEG/MMT-20 nanocomposite

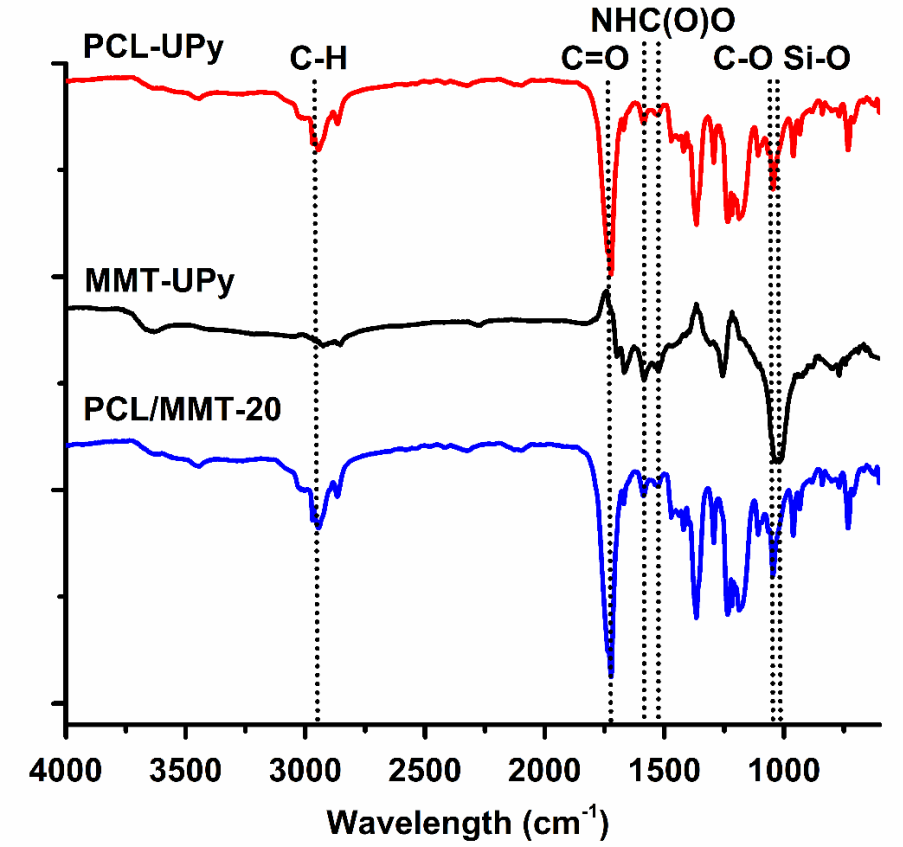

Figure 4.5 : FT-IR spectra ofneat PCL-UPy, MMT-UPy and PCL/MMT-20 nanocomposite

The FTIR spectra of the two samples clearly exhibited the characteristic absorptions bands that were attributable to PEG-UPy, PCL-UPy and MMT-UPy. The characteristic bands of PEG-UPy (3320 (N-H), 2875 (C-H), 1700 (UPy), 1670 (UPy), 1620 (urea), 1580 (UPy), 1530 (UPy), 1185 (C–O stretch)) and PCL-UPy (3320 (N-H), 2940 (C-H), 2865 (C-H), 1720 (C=O stretch), 1700 (UPy), 1670 (UPy), 1620 (urea), 1580 (UPy), 1530 (UPy), 1185 (C–O stretch)) samples appeared in these spectra with insignificant shifting. The new band that appeared in the region of 1040 cm^{-1} was attributed to Si-O stretching band of MMT-UPy and was indicating the existence of nanoclays in the polymer matrices where the polymer chain was inserted between the layers of the MMT by multiple hydrogen bonding interactions.

4.2.4 The morphology of PEG/MMT and PCL/MMT nanocomposites

The XRD, DSC and TGA results of PEG/MMT and PCL/MMT nanocomposites with various nanoclay loadings were collected in Table 4.1. After the nanocomposites formation, the XRD peak of MMT-UPy (4.75°) disappeared in the diffraction patterns of the nanocomposites with 3 and 5% loadings, which indicated the formation of exfoliated structures. In addition, the PEG/MMT-10, PEG/MMT-20, PCL/MMT-10 and PCL/MMT-20 samples exhibited small and broad peaks that might be resulting from partially exfoliated or intercalated structures with d-spacings of 3.69, 3.74, 3.91 and 3.96 nm, respectively. The amount of clay in the polymer matrix is an important parameter for the complete exfoliation. By increasing clay contents, the agglomerated structures became denser in the polymer matrix and it could be more difficult to overcome the intensive ionic attraction between the neighboring platelets[57].

Table 4.1 : Physical properties of PEG/MMT and PCL/MMT nanocomposites and their components for comparison.

Entry	d_{001}[a] (nm)	T_m[b] (°C)	Weight losstemperature[c](°C)		Char yield[c] (%)
			%10	%50	
MMT-	1.82	-	570	-	79.7
MMT-UPy	1.87	-	256	-	57.3
PEG-UPy	-	54.7	328	389	-
PCL-UPy	-	57.5	338	388	-
PEG/MMT-3	n.d.[e]	54.9	333	394	2.0
PEG/MMT-5	n.d.	55.3	341	397	4.8
PEG/MMT-10	3.69	55.5	344	400	9.6
PEG/MMT-20	3.74	55.6	353	404	18.7
PCL/MMT-3	n.d.	58.1	355	390	2.7
PCL/MMT-5	n.d.	58.8	360	393	4.2
PCL/MMT-10	3.91	59.4	366	399	9.4
PCL/MMT-20	3.96	59.9	371	404	18.2

[a]Basal spacing (d_{001}) is calculated by XRD analysis. [b]Determined by DSC and analyses under a nitrogen flow at a heating rate of 10 °C/min. [c]Determined by TGA analysis under a nitrogen flow at a heating rate of 10 °C/min. [e]Probably complete exfoliated nanocomposites.

The XRD analysis is a useful screening tool for determining if any sort of nanocomposites, but its reliability is limited due to the clay dilution, preferred orientation, mixed layering and other peak broadening factors. It can be used with direct imaging techniques such as atomic force microscopy (AFM), scanning

electron microscopy (SEM) or transmission electron microscopy (TEM) to define the exact nature of the nanocomposites. TEM images of selected PEG/MMT-5 nanocomposite were provided in Figure 4.6 at different magnifications. The silicate layers appear as dark grey lines about 1.0 nm thick and from 50 to 100 nm in lateral dimension and the gray/white areas represent the polymer matrix.

The low magnification TEM image (Figure 4.6a) clearly showed that most silicate layers were exfoliated and dispersed in the polymer matrix homogenously. Moreover, the intercalated silicate layers were locally stacked in some regions of polymer matrix. The low magnification image showed the general dispersion of silicate layers in the polymer matrix, whereas a high magnification image (Figure 4.6b) clearly identified multi-layer platelets of organoclay.

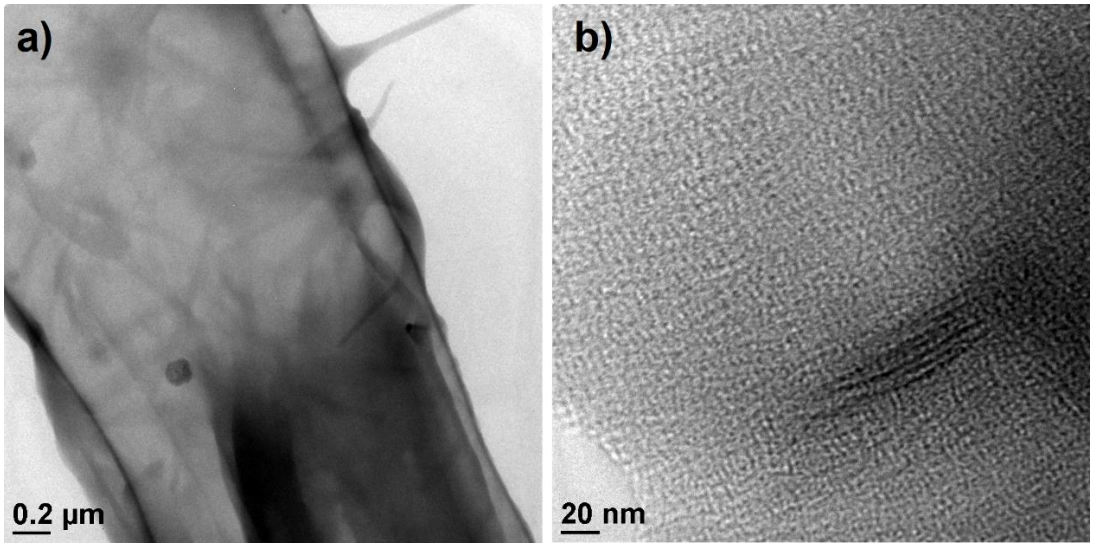

Figure 4.6 : TEM micrographs of PEG/MMT-5 in low (a, scale bar: 200 nm) and high (b, scale bar: 20 nm) magnifications.

The TEM images of PCL/MMT also displayed the mixed morphologies including intercalated layers with a non-uniform separation and exfoliated single layers isolated from any stack (Figure 4.7). Although it was not detected a peak in the XRD pattern for this sample, there was still intercalated structure in this sample. Combined together with XRD and TEM results, it could be concluded that partially exfoliated/intercalated structures were achieved in all nanocomposites. The coexistence of mixed morphologies implied that the van der Waals force and Coulombic force between intergalleries were still strong to hold them tightly. Therefore, some of the silicate layers could not to be separated completely. Besides, the silicate layers have high specific surface area and surface energy, which may also

make them tend to aggregate together rather than to disperse homogeneously in the polymer matrix, especially at high clay loadings[20].

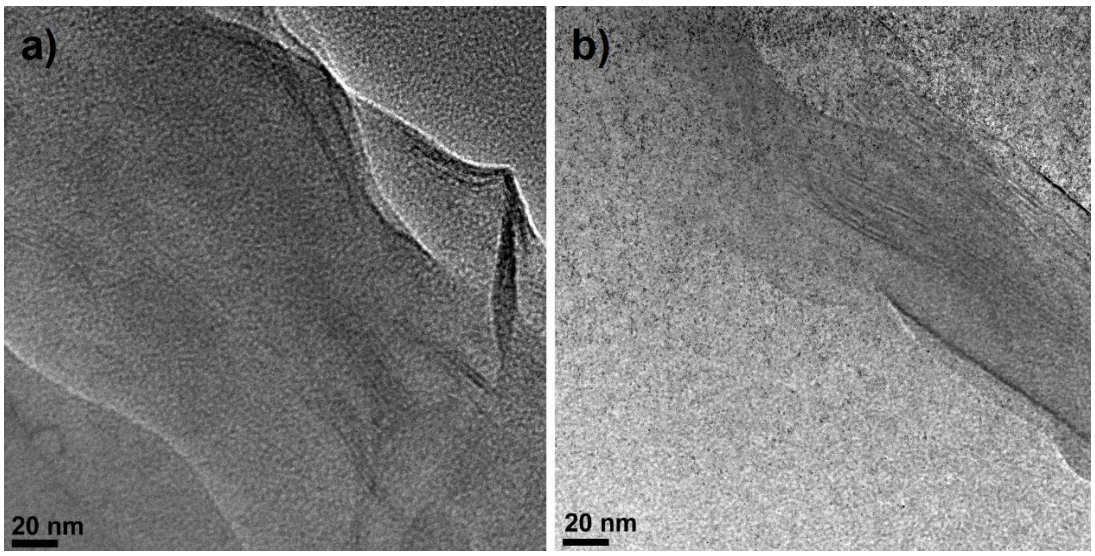

Figure 4.7 : TEM micrographs of PCL/MMT-5 in high (scale bar: 20 nm) magnification.

4.2.5 Thermal behavior

Thermal behaviors of the nanocomposites were investigated by TGA and DSC analyses. Thermal stability of the nanocomposites was studied by TGA, heating from room temperature to 800 ^{o}C under nitrogen atmosphere to avoid thermal oxidation and to establish a more direct correlation between chemical structure and thermal degradation. The TGA results showed that all PEG/MMT samples degraded through single degradation step in the temperature range 200-450 ^{o}C (Figure 4.8). Thermal degradation begins at 200 ^{o}C, consistent with the degradation of UPy moieties, and accelerated at 290 ^{o}C as the PEG chains began to degrade. In order to establish the influence of the MMT content on the thermal stability of PEG, the T_{onset} (temperature at 10% weight loss) and T_{max} (temperature at 50% weight loss) were collected in Table 4.1. Both T_{onset} and T_{max} values of PEG/MMT samples increased almost linearly by increasing clay contents. It was clearly found that both degradation temperatures of all nanocomposites shifted significantly toward higher temperatures compared to those of the neat PEG.

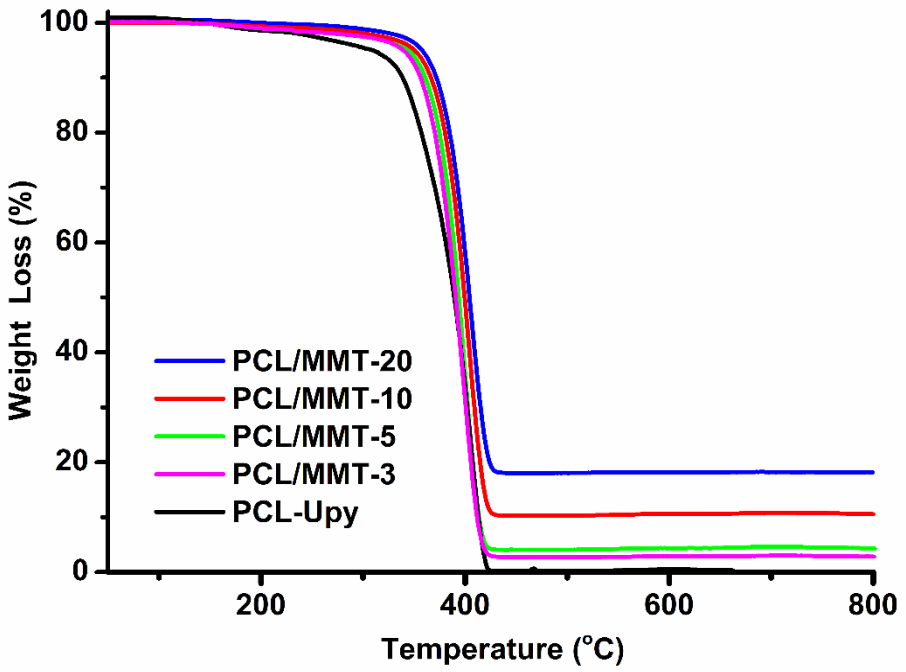

Figure 4.8 : TGA thermograms of neat PEG-UPy and resulting nanocomposites containing 3, 5, 10 and 20 % MMT-UPy.

The influence of MMT on the thermal stability of PCL was also investigated for the heating rate 10°C/min since a similar behavior was observed for all samples. From the TGA results, it was clear that T_{onset} and T_{max} temperatures of all samples moved significantly toward a higher temperature compared to those of the pristine polymer. Figure 4.9 confirmed that PCL/MMT nanocomposites displayed two-step mechanism of degradation containing simultaneous random chain scission and depolymerization. In the first step, pyrolysis of the ester groups which was associated with random chain scission led to release of CO_2, H_2O and hexanoic acid. For the second step, ε-caprolactone was formed as a product of an unzipping depolymerization process. The remaining mass after all organic material has been burned away gives the char yields of the nanocomposites. The char yields at 800 °C for both PEG/MMT and PCL/MMT samples were increased by increasing the clay loadings. These results demonstrated good control over clay contents in the nanocomposites. The increase in char yield also proved the reduction of the polymer's flammability and implies good thermal stability. The final char yield of all PCL/MMT nanocomposites was improved by increasing the clay contents. The increase in char yield indicates the reduction of the polymer's flammability and implies good thermal stability[79].

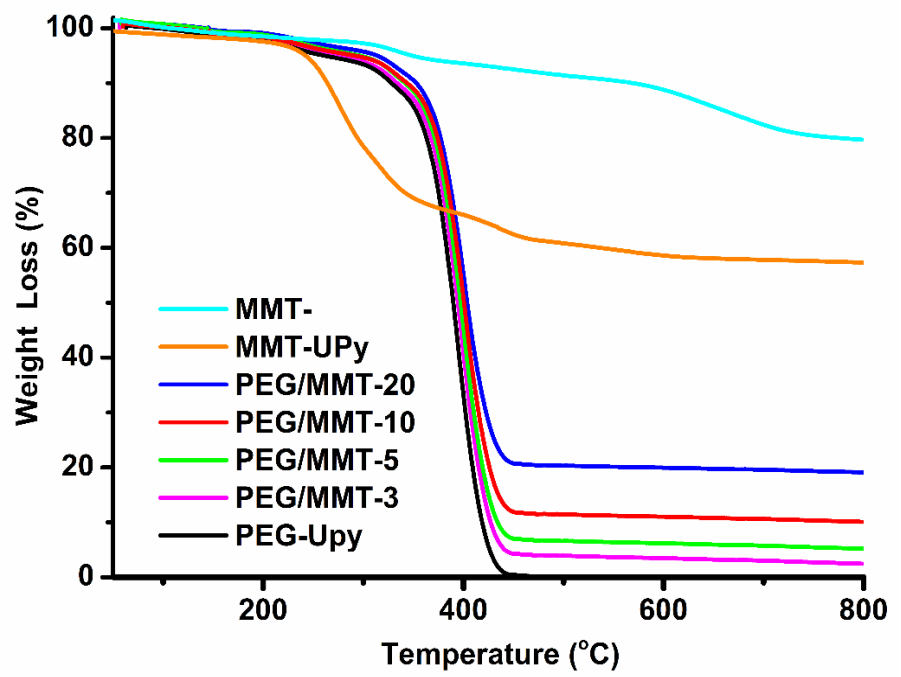

Figure 4.9 : TGA thermograms of neat PCL-UPy and resulting nanocomposites containing 3, 5, 10 and 20 % MMT-UPy.

Differential scanning calorimetry (DSC) analyses of neat polymers and all nanocomposites samples were carried out to determine melting temperature (T_m) values at various clay loadings (Table 4.1). Figure 4.10 showed that samples up to 20 wt% of MMT have one endothermic peak which represents melting of the crystalline phase in both PEG (54.7 ^oC) and PCL (57.5 ^oC) semi-crystalline polymers. It was founded that clay loadings have no significant effect on the T_m of the nanocomposites. The nanocomposites showed a slight increase in T_m with increasing clay loadings, suggesting that the presence of silicate layers and UPy motifs led to accelerate crystalline structures in the nanocomposites formation. This observation could be attributed to the confinement of the intercalated polymer chains within the clay galleries, which prevents the segmental motions of the polymer chains. Moreover, the UPy motifs could also act as physical crosslinks and thereby increase T_m. This slight increase in crystallinity has also been observed in traditional polymer nanocomposites and reported by other groups[80, 81].

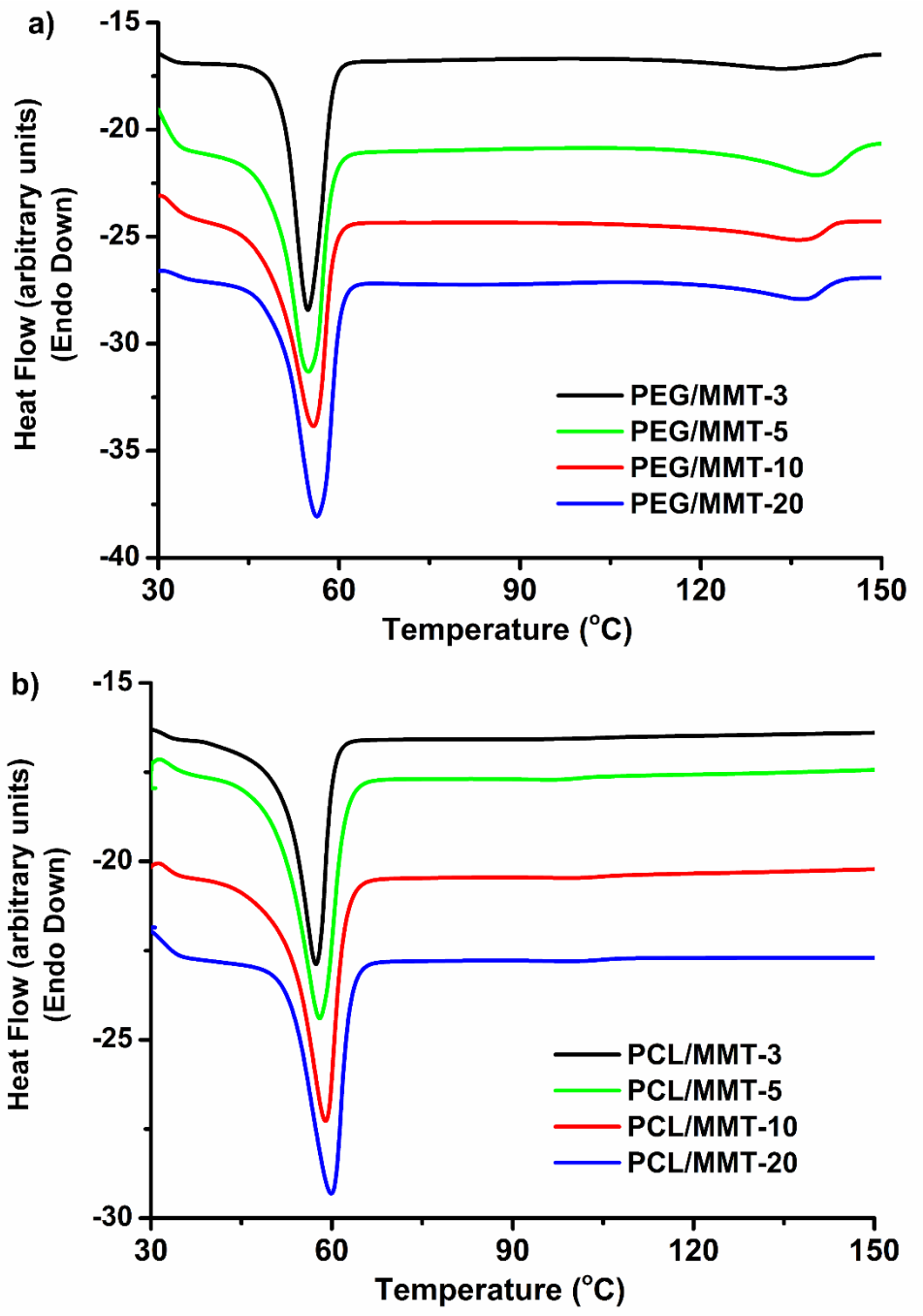

Figure 4.10 : DSC traces of a) neat PEG-UPy and resulting nanocomposites b) neat PCL-UPy and resulting nanocomposites.

4.3 Conclusions

The organomodified clay containing self-complementary UPy motifs was successfully prepared and its structure was determined by XRD, TGA and FT-IR analyses. A series of PEG/MMT and PCL/MMT nanocomposites have been prepared by solution blending with various clay loadings. The combined XRD and TEM

results confirmed that all nanocomposites have a complex morphology with partial intercalation/exfoliation. According to TGA results, T_{onset} and T_{max} temperatures of the nanocomposites were greater than that of pristine polymers. On the other hand, T_m values of nanocomposites slightly improved by increasing clay loadings, suggesting that the addition of clay did not affect the crystallinity of the both PEG and PCL semi-crystalline polymers.

5. CONCLUSIONS

Polymer nanocomposites are hybrid organic-inorganic materialswith at least onedimension of the filler phase less than 100nm. There are three main routes for the preparation of polymer/clay nanocomposites including melt intercalation, solution exfoliation and *in-situ* polymerization. Among them, the*in-situ* polymerization has several advantages.First of all,thermoplastic- and thermoset-based nanocomposites can be synthesized via this route. In addition, it permits the grafting of polymers on filler surface,which can generally improve properties of the final composite. Three types of microstructure,unintercalated (or microcomposite),intercalated (and/or flocculated), or exfoliated (or delaminated) are obtained based on the method and materials used.The main aim of this thesis is conceived to greatly extend the preparation of polymer/clay nanocompositesby careful choices of efficient synthetic reaction using suitable organic clays and polymers, and the optimization of these processes to deliver the biggest benefit.

In the first part of the thesis,a series of polystyrene/clay nanocomposites were prepared via a highly efficient atom transfer nitroxide radical coupling (ATNRC) chemistry which, is based on mixing a nitroxide-containing organoclay with corresponding halide-containing polystyrene in the presence of CuCl/PMDETA catalytic system.Spectroscopic and microscopic investigations revealed that successful nanocomposite formation has been achieved by this method. By addition of small amounts of layered silicate loadings resulted in remarkable improvements of thermal properties of nanocomposites.

In the second part of the thesis,the preparation of A_3-type star poly(methylmethacrylate)/clay nanocomposites were achieved by in-situ ATRP initiated from organomodified montmorillonite containing quaternary trifunctional ATRP initiator. Linear kinetic plot and increase in molecular weight with conversion indicated that ATRP of MMA was controlled. Spectroscopic and microscopic investigations revealed a complex morphology, with partial intercalation/exfoliation, which depends on the concentration of clay.The exfoliated nanocomposite has been

obtained when polymerization was conducted with 1% of organic clay loading. However, with increasing the clay loading to 3, 6 and 10%, the degree of exfoliation of the nanocomposites decreased, which confirmed by both XRD and TEM analyses. This may be due to short chain length of branches of the star polymer. The DSC and TGA analyses showed that all nanocomposites have higher Tg value and thermal stabilities compared to neat poly(methyl methacrylate).

In the last part of the thesis,the preparation of polymer/clay nanocomposites by specific hydrogen bonding interactions between surface functionalized silica nanoclays and 2-ureido-4[1H]pyrimidinone-bonded supramolecular poly(ethylene glycol) or poly(ε-caprolactone)s, which has self-association capability through quadruple hydrogen bonds. Various PEG/MMT and PCL/MMT nanocomposites containing different clay loadingshave been prepared by solution blending with UPy-MMT clay andUPy-terminated poly(ethylene glycol) or poly(ε-caprolactone). The combined XRD and TEM results confirmed that all nanocomposites have a complex morphology with partial intercalation/exfoliation. According to TGA results, T_{onset} andT_{max} temperatures of the nanocomposites were greater than that of pristine polymers. On the other hand, T_m values of nanocomposites slightly improved by increasing clay loadings, suggesting that the addition of clay did not affect the crystallinity of the both PEG and PCL semi-crystalline polymers.

We also make recommendation that further research remain to be carried out to exploredifferent efficient synthesis techniques using various nanoclays and polymers to yieldnovel polymer/clay nanocomposites improving pure polymer properties. Comparison experiment by other techniques like solution exfoliation or melt intercalation for mixing ofpolymer and nanoclayscan be carried out to seehow the clay layerspossibly dispersed in the polymer matrices. Characterization of of final nanocomposites using spectroscopic and microscopic analyses may give a better description of the degree of dispersion. Testing of mechanicalproperties including tensile and impact can be studied to verify the improvents due tothe inclusion of clay nanoparticles. Other vinyl monomers such as acrylonitrile or vinyl chloride and othernanopowders such as SiO_2, POSS, halloysite which are limited investigated yet will be a vast range of possibilities to be explored by using surfacemodification with silane coupling agents and *in-situ* polymerization strategy we proposed here.

REFERENCES

[1] **Alexandre, M. and Dubois, P.** (2000). Polymer-layered silicate nanocomposites: Preparation, properties and uses of a new class of materials. *Materials Science & Engineering R-Reports*, 28, 1-63.

[2] **Ray, S.S. and Okamoto, M.** (2003). Polymer/layered silicate nanocomposites: A review from preparation to processing. *Progress in Polymer Science*, 28, 1539-1641.

[3] **Pavlidou, S. and Papaspyrides, C.D.** (2008). A review on polymer-layered silicate nanocomposites. *Progress in Polymer Science*, 33, 1119-1198.

[4] **Tasdelen, M.A., Kreutzer, J., and Yagci, Y.** (2010). In situ synthesis of polymer/clay nanocomposites by living and controlled/living polymerization. *Macromolecular Chemistry and Physics*, 211, 279-285.

[5] **Akat, H., Tasdelen, M.A., Du Prez, F., and Yagci, Y.** (2008). Synthesis and characterization of polymer/clay nanocomposites by intercalated chain transfer agent. *European Polymer Journal*, 44, 1949-1954.

[6] **Oral, A., Tasdelen, M.A., Demirel, A.L., and Yagci, Y.** (2009). Poly(cyclohexene oxide)/clay nanocomposites by photoinitiated cationic polymerization via activated monomer mechanism. *Journal of Polymer Science Part a-Polymer Chemistry*, 47, 5328-5335.

[7] **Yenice, Z., Tasdelen, M.A., Oral, A., Guler, C., and Yagci, Y.** (2009). Poly(styrene-b-tetrahydrofuran)/clay nanocomposites by mechanistic transformation. *Journal of Polymer Science Part a-Polymer Chemistry*, 47, 2190-2197.

[8] **Eksik, O., Tasdelen, M.A., Erciyes, A.T., and Yagci, Y.** (2010). In situ synthesis of oil-based polymer/silver nanocomposites by photoinduced electron transfer and free radical polymerization processes. *Composite Interfaces*, 17, 357-369.

[9] **Altinkok, C., Uyar, T., Tasdelen, M.A., and Yagci, Y.** (2011). In situ synthesis of polymer/clay nanocomposites by type ii photoinitiated free radical polymerization. *Journal of Polymer Science Part a-Polymer Chemistry*, 49, 3658-3663.

[10] **Demir, K.D., Tasdelen, M.A., Uyar, T., Kawaguchi, A.W., Sudo, A., Endo, T., and Yagci, Y.** (2011). Synthesis of polybenzoxazine/clay nanocomposites by in situ thermal ring-opening polymerization using intercalated monomer. *Journal of Polymer Science Part a-Polymer Chemistry*, 49, 4213-4220.

[11] **Dizman, C., Ates, S., Uyar, T., Tasdelen, M.A., Torun, L., and Yagci, Y.** (2011). Polysulfone/clay nanocomposites by in situ photoinduced crosslinking polymerization. *Macromolecular Materials and Engineering*, 296, 1101-1106.

[12] **Nese, A., Sen, S., Tasdelen, M.A., Nugay, N., and Yagci, Y.** (2006). Clay-pmma nanocomposites by photoinitiated radical polymerization using intercalated phenacyl pyridinium salt initiators. *Macromolecular Chemistry and Physics*, 207, 820-826.

[13] **Huskic, M., Zagar, E., and Zigon, M.** (2012). The influence of a quaternary ammonium salt and mmt on the in situ intercalative polymerization of pmma. *European Polymer Journal*, 48, 1555-1560.

[14] **Huskic, M. and Zigon, M.** (2007). Pmma/mmt nanocomposites prepared by one-step in situ intercalative solution polymerization. *European Polymer Journal*, 43, 4891-4897.

[15] **Datta, H., Bhowmick, A.K., and Singha, N.K.** (2008). Tailor-made hybrid nanostructure of poly(ethyl acrylate)/clay by surface-initiated atom transfer radical polymerization. *Journal of Polymer Science Part a-Polymer Chemistry*, 46, 5014-5027.

[16] **Haloi, D.J. and Singha, N.K.** (2011). Synthesis of poly(2-ethylhexyl acrylate)/clay nanocomposite by in situ living radical polymerization. *Journal of Polymer Science Part a-Polymer Chemistry*, 49, 1564-1571.

[17] **Kolb, H.C., Finn, M.G., and Sharpless, K.B.** (2001). Click chemistry: Diverse chemical function from a few good reactions. *Angewandte Chemie-International Edition*, 40, 2004-2021.

[18] **Tasdelen, M.A., Van Camp, W., Goethals, E., Dubois, P., Du Prez, F., and Yagci, Y.** (2008). Polytetrahydrofuran/clay nanocomposites by in situ polymerization and "click" chemistry processes. *Macromolecules*, 41, 6035-6040.

[19] **Oral, A., Tasdelen, M.A., Demirel, A.L., and Yagci, Y.** (2009). Poly(methyl methacrylate)/clay nanocomposites by photoinitiated free radical polymerization using intercalated monomer. *Polymer*, 50, 3905-3910.

[20] **Tasdelen, M.A.** (2011). Poly(epsilon-caprolactone)/clay nanocomposites via "click" chemistry. *European Polymer Journal*, 47, 937-941.

[21] **Ye, Y.S., Yen, Y.C., Cheng, C.C., Syu, Y.J., Huang, Y.J., and Chang, F.C.** (2010). Polytriazole/clay nanocomposites synthesized using in situ polymerization and click chemistry. *Polymer*, 51, 430-436.

[22] **Chen, J.C., Wang, H.D., Luo, W.Q., Xiang, J.M., Zhang, L.H., and Sun, B.B.** (2010). Preparation of poly(epsilon-caprolactone)@attapulgite nanocomposites via a combination of controlled ring-opening polymerization and click chemistry. *Colloid and Polymer Science*, 288, 173-179.

[23] **Chen, J.C., Xiang, J.M., Cai, Z.W., Yong, H., Wang, H.D., Zhang, L.H., Luo, W.Q., and Min, H.** (2010). Synthesis of hydrophobic polymer brushes on silica nanoparticles via the combination of surface-initiated atrp, rop and click chemistry. *Journal of Macromolecular Science Part a-Pure and Applied Chemistry*, 47, 655-662.

[24] **Fu, Q., Lin, W., and Huang, J.** (2008). A new strategy for preparation of graft copolymers via "graft onto" by atom transfer nitroxide radical coupling chemistry: Preparation of poly(4-glycidyloxy-2,2,6,6-tetramethylpiperidine-1-oxyl-co-ethylene oxide)-graft-polystyrene and poly(tert-butyl acrylate). *Macromolecules*, 41, 2381-2387.

[25] **Fu, Q., Liu, C., Lin, W., and Huang, J.** (2008). One-pot synthesis of heterograft copolymers via "graft onto" by atom transfer nitroxide radical coupling chemistry. *Journal of Polymer Science Part a-Polymer Chemistry*, 46, 6770-6779.

[26] **Liu, C., Pan, M., Zhang, Y., and Huang, J.** (2008). Preparation of star block copolymers with polystyrene-block-poly(ethylene oxide) as side chains on hyperbranched polyglycerol core by combination of atrp with atom transfer nitroxide radical coupling reaction. *Journal of Polymer Science Part a-Polymer Chemistry*, 46, 6754-6761.

[27] **Fu, Q., Wang, G., Lin, W., and Huang, J.** (2009). One-pot preparation of 3-miktoarm star terpolymers via "click chemistry" and atom transfer nitroxide radical coupling reaction. *Journal of Polymer Science Part a-Polymer Chemistry*, 47, 986-990.

[28] **Fu, Q., Wang, G.W., Lin, W.C., and Huang, J.L.** (2009). One-pot preparation of 3-miktoarm star terpolymers via "click chemistry" and atom transfer nitroxide radical coupling reaction. *Journal of Polymer Science Part a-Polymer Chemistry*, 47, 986-990.

[29] **Deng, Y., Li, Y., Dai, J., Lang, M., and Huang, X.** (2011). An efficient way to functionalize graphene sheets with presynthesized polymer via atnrc chemistry. *Journal of Polymer Science Part a-Polymer Chemistry*, 49, 1582-1590.

[30] **Jockusch, S., Zeika, O., Jayaraj, N., Ramamurthy, V., and Turro, N.J.** (2010). Electron spin polarization transfer from a nitroxide incarcerated within a nanocapsule to a nitroxide in the bulk aqueous solution. *Journal of Physical Chemistry Letters*, 1, 2628-2632.

[31] **Sanchez, C., Soler-Illia, G., Ribot, F., Lalot, T., Mayer, C.R., and Cabuil, V.** (2001). Designed hybrid organic-inorganic nanocomposites from functional nanobuilding blocks. *Chemistry of Materials*, 13, 3061-3083.

[32] **Balazs, A.C., Emrick, T., and Russell, T.P.** (2006). Nanoparticle polymer composites: Where two small worlds meet. *Science*, 314, 1107-1110.

[33] **Giannelis, E.P.** (1996). Polymer layered silicate nanocomposites. *Advanced Materials*, 8, 29-&.

[34] **Roghani-Mamaqani, H., Haddadi-Asl, V., and Salami-Kalajahi, M.** (2012). In situ controlled radical polymerization: A review on synthesis of well-defined nanocomposites. *Polymer Reviews*, 52, 142-188.

[35] **Aydin, M., Tasdelen, M.A., Uyar, T., Jockusch, S., Turro, N.J., and Yagci, Y.** (2013). Polystyrene/clay nanocomposites by atom transfer radical nitroxide coupling chemistry. *Journal of Polymer Science Part a-Polymer Chemistry*, 51, 1024-1028.

[36] **Huskic, M. and Zigon, M.** (2009). The effects of experimental parameters on the extent of intercalation of pmma/mmt nanocomposites prepared in solution. *Journal of Applied Polymer Science*, 113, 1182-1187.

[37] **Zhao, H.Y., Argoti, S.D., Farrell, B.P., and Shipp, D.A.** (2004). Polymer-silicate nanocomposites produced by in situ atom transfer radical polymerization. *Journal of Polymer Science Part a-Polymer Chemistry*, 42, 916-924.

[38] **Bottcher, H., Hallensleben, M.L., Nuss, S., Wurm, H., Bauer, J., and Behrens, P.** (2002). Organic/inorganic hybrids by 'living'/controlled atrp grafting from layered silicates. *Journal of Materials Chemistry*, 12, 1351-1354.

[39] **Tasdelen, M.A. and Yagci, Y.** (2011). Photochemical methods for the preparation of complex linear and cross-linked macromolecular structures. *Australian Journal of Chemistry*, 64, 982-991.

[40] **Zhao, H.Y., Farrell, B.P., and Shipp, D.A.** (2004). Nanopatterns of poly (styrene-block-butyl acrylate) block copolymer brushes on the surfaces of exfoliated and intercalated clay layers. *Polymer*, 45, 4473-4481.

[41] **Di, J. and Sogah, D.Y.** (2006). Exfoliated block copolymer/silicate nanocomposites by one-pot, one-step in-situ living polymerization from silicate-anchored multifunctional initiator. *Macromolecules*, 39, 5052-5057.

[42] **Singha, N.K., Kavitha, A., Haloi, D.J., Mandal, P., Janke, A., Jehnichen, D., Komber, H., and Voit, B.** (2012). Effect of nanoclay on in situ preparation of "all acrylate" aba triblock copolymers via atrp and their morphology. *Macromolecular Chemistry and Physics*, 213, 2034-2043.

[43] **Haloi, D.J., Ata, S., and Singha, N.K.** (2012). Synthesis and characterization of all acrylic block copolymer/clay nanocomposites prepared via surface initiated atom transfer radical polymerization (si-atrp). *Industrial & Engineering Chemistry Research*, 51, 9760-9768.

[44] **Zhao, H.Y. and Shipp, D.A.** (2003). Preparation of poly(styrene-block-butyl acrylate) block copolymer-silicate nanocomposites. *Chemistry of Materials*, 15, 2693-2695.

[45] **Bae, W.J., Kim, K.H., Jo, W.H., and Park, Y.H.** (2004). Exfoliated nanocomposite from polyaniline graft copolymer/clay. *Macromolecules*, 37, 9850-9854.

[46] **Raquez, J.-M., Nabar, Y., Narayan, R., and Dubois, P.** (2011). Preparation and characterization of maleated thermoplastic starch-based nanocomposites. *Journal of Applied Polymer Science*, 122, 639-647.

[47] **Maji, P.K., Guchhait, P.K., and Bhowmick, A.K.** (2009). Effect of the microstructure of a hyperbranched polymer and nanoclay loading on the morphology and properties of novel polyurethane nanocomposites. *Acs Applied Materials & Interfaces*, 1, 289-300.

[48] **Deka, H. and Karak, N.** (2009). Vegetable oil-based hyperbranched thermosetting polyurethane/clay nanocomposites. *Nanoscale Research Letters*, 4, 758-765.

[49] **Deka, H. and Karak, N.** (2011). Bio-based hyperbranched polyurethane/clay nanocomposites: Adhesive, mechanical, and thermal properties. *Polymers for Advanced Technologies*, 22, 973-980.

[50] **Deka, H. and Karak, N.** (2010). Influence of highly branched poly(amido amine) on the properties of hyperbranched polyurethane/clay nanocomposites. *Materials Chemistry and Physics*, 124, 120-128.

[51] **Singh, C. and Balazs, A.C.** (2000). Effect of polymer architecture on the miscibility of polymer/clay mixtures. *Polymer International*, 49, 469-471.

[52] **Robello, D.R., Yamaguchi, N., Blanton, T., and Barnes, C.** (2004). Spontaneous formation of an exfoliated polystyrene-clay nanocomposite using a star-shaped polymer. *Journal of the American Chemical Society*, 126, 8118-8119.

[53] **Li, Y.T., Narain, R., Ma, Y.H., Lewis, A.L., and Armes, S.P.** (2004). Biomimetic thermo-responsive star diblock gelators. *Chemical Communications*, 2746-2747.

[54] **Pandey, J.K., Reddy, K.R., Kumar, A.P., and Singh, R.P.** (2005). An overview on the degradability of polymer nanocomposites. *Polymer Degradation and Stability*, 88, 234-250.

[55] **Okada, A. and Usuki, A.** (2006). Twenty years of polymer-clay nanocomposites. *Macromolecular Materials and Engineering*, 291, 1449-1476.

[56] **Aydin, M., Tasdelen, M.A., Uyar, T., and Yagci, Y.** (2013). In situ synthesis of a(3)-type star polymer/clay nanocomposites by atom transfer radical polymerization. *Journal of Polymer Science Part a-Polymer Chemistry*, 51, 5257-5262.

[57] **Barlas, F.B., Seleci, D.A., Ozkan, M., Demir, B., Seleci, M., Aydin, M., Tasdelen, M.A., Zareie, H.M., Timur, S., Ozcelik, S., and Yagci, Y.** (2014). Folic acid modified clay/polymer nanocomposites for selective cell adhesion. *Journal of Materials Chemistry B*, 2, 6412-6421.

[58] **Bongiovanni, R., Turcato, E.A., Di Gianni, A., and Ronchetti, S.** (2008). Epoxy coatings containing clays and organoclays: Effect of the filler and its water content on the uv-curing process. *Progress in Organic Coatings*, 62, 336-343.

[59] **Ceccia, S., Turcato, E.A., Maffettone, P.L., and Bongiovanni, R.** (2008). Nanocomposite uv-cured coatings: Organoclay intercalation by an epoxy resin. *Progress in Organic Coatings*, 63, 110-115.

[60] **Di Gianni, A., Amerio, E., Monticelli, O., and Bongiovanni, R.** (2008). Preparation of polymer/clay mineral nanocomposites via dispersion of silylated montmorillonite in a uv curable epoxy matrix. *Applied Clay Science*, 42, 116-124.

[61] **Di Gianni, A., Bongiovanni, R., Conzatti, L., and Turri, S.** (2009). New fluorinated montmorillonites for the preparation of uv-cured coatings. *Journal of Colloid and Interface Science*, 336, 455-461.

[62] **Malucelli, G., Bongiovanni, R., Sangermano, M., Ronchetti, S., and Priola, A.** (2007). Preparation and characterization of uv-cured epoxy nanocomposites based on o-montmorillonite modified with maleinized liquid polybutadienes. *Polymer*, 48, 7000-7007.

[63] **Huskic, M., Zigon, M., and Ivankovic, M.** (2013). Comparison of the properties of clay polymer nanocomposites prepared by montmorillonite modified by silane and by quaternary ammonium salts. *Applied Clay Science*, 85, 109-115.

[64] **Schreiber, F.** (2000). Structure and growth of self-assembling monolayers,*Progress in Surface Science*, 65, 151-256.

[65] **Whitesides, G.M., Mathias, J.P., and Seto, C.T.** (1991). Molecular self-assembly and nanochemistry - a chemical strategy for the synthesis of nanostructures. *Science*, 254, 1312-1319.

[66] **Sontjens, S.H.M., Sijbesma, R.P., van Genderen, M.H.P., and Meijer, E.W.** (2000). Stability and lifetime of quadruply hydrogen bonded 2-ureido-4 1h -pyrimidinone dimers. *Journal of the American Chemical Society*, 122, 7487-7493.

[67] **Feldman, K.E., Kade, M.J., de Greef, T.F.A., Meijer, E.W., Kramer, E.J., and Hawker, C.J.** (2008). Polymers with multiple hydrogen-bonded end groups and their blends. *Macromolecules*, 41, 4694-4700.

[68] **ten Cate, A.T., Kooijman, H., Spek, A.L., Sijbesma, R.P., and Meijer, E.W.** (2004). Conformational control in the cyclization of hydrogen-bonded supramolecular polymers. *Journal of the American Chemical Society*, 126, 3801-3808.

[69] **Guo, M., Pitet, L.M., Wyss, H.M., Vos, M., Dankers, P.Y.W., and Meijer, E.W.** (2014). Tough stimuli-responsive supramolecular hydrogels with hydrogen-bonding network junctions. *Journal of the American Chemical Society*, 136, 6969-6977.

[70] **Delgado, P.A. and Hillmyer, M.A.** (2014). Combining block copolymers and hydrogen bonding for poly(lactide) toughening. *Rsc Advances*, 4, 13266-13273.

[71] **Botterhuis, N.E., van Beek, D.J.M., van Gemert, G.M.L., Bosman, A.W., and Sijbesma, R.P.** (2008). Self-assembly and morphology of polydimethylsiloxane supramolecular thermoplastic elastomers. *Journal of Polymer Science Part a-Polymer Chemistry*, 46, 3877-3885.

[72] **Wrue, M.H., McUmber, A.C., and Anthamatten, M.** (2009). Atom transfer radical polymerization of end-functionalized hydrogen-bonding polymers and resulting polymer miscibility. *Macromolecules*, 42, 9255-9262.

[73] **McKee, M.G., Elkins, C.L., Park, T., and Long, T.E.** (2005). Influence of random branching on multiple hydrogen bonding in poly(alkyl methacrylate)s. *Macromolecules*, 38, 6015-6023.

[74] **Folmer, B.J.B., Sijbesma, R.P., Versteegen, R.M., van der Rijt, J.A.J., and Meijer, E.W.** (2000). Supramolecular polymer materials: Chain extension of telechelic polymers using a reactive hydrogen-bonding synthon. *Advanced Materials*, 12, 874-878.

[75] **Kowalski, A., Duda, A., and Penczek, S.** (2000). Mechanism of cyclic ester polymerization initiated with tin(ii) octoate. 2. Macromolecules fitted with tin(ii) alkoxide species observed directly in maldi-tof spectra. *Macromolecules*, 33, 689-695.

[76] **Neikirk, C.C., Chung, J.W., and Priestley, R.D.** (2013). Thermomechanical behavior of hydrogen-bond based supramolecular poly(epsilon-caprolactone)-silica nanocomposites. *Rsc Advances*, 3, 16686-16696.

[77] **Bobade, S., Wang, Y., Mays, J., and Baskaran, D.** (2014). Synthesis and characterization of ureidopyrimidone telechelics by cuaac "click" reaction: Effect of t-g and polarity. *Macromolecules*, 47, 5040-5050.

[78] **van Beek, D.J.M., Spiering, A.J.H., Peters, G.W.M., te Nijenhuis, K., and Sijbesma, R.P.** (2007). Unidirectional dimerization and stacking of ureidopyrimidinone end groups in polycaprolactone supramolecular polymers. *Macromolecules*, 40, 8464-8475.

[79] **Leszczyńska, A., Njuguna, J., Pielichowski, K., and Banerjee, J.R.** (2007). Polymer/montmorillonite nanocomposites with improved thermal properties: Part i. Factors influencing thermal stability and mechanisms of thermal stability improvement. *Thermochimica Acta*, 453, 75-96.

[80] **Lepoittevin, B., Devalckenaere, M., Pantoustier, N., Alexandre, M., Kubies, D., Calberg, C., Jérôme, R., and Dubois, P.** (2002). Poly(ε-caprolactone)/clay nanocomposites prepared by melt intercalation: Mechanical, thermal and rheological properties. *Polymer*, 43, 4017-4023.

[81] **Homminga, D., Goderis, B., Dolbnya, I., Reynaers, H., and Groeninckx, G.** (2005). Crystallization behavior of polymer/montmorillonite nanocomposites. Part i. Intercalated poly(ethylene oxide)/montmorillonite nanocomposites. *Polymer*, 46, 11359-11365.

CURRICULUM VITAE

Name Surname: Muhammed AYDIN

Place and Date of Birth: Adilcevaz-1980

E-Mail: aydinmuhammed@gmail.com

Universityand College Degreesobtained:

2009 – 2015 Philosophy of Doctorate

Chemistry, Istanbul Technical University, Graduate School of Science Engineering and Technology

2005 – 2009 Master of Science

Chemistry, Istanbul Technical University, Graduate School of Science Engineering and Technology

2000 – 2004 Bachelor of Science

Chemistry, Faculty of Art and Sciences, Mustafa Kemal University

Professional Experience and Awards:

2008 - 2014 Research Assistant, Chemistry, Istanbul Technical University

Publications from thesis:

- **Aydin M.**, Tasdelen M. A., Uyar T., Jockusch S., Turro, N.J., and Yagci, Y., Polystyrene/clay Nanocomposites by Atom Transfer Radical Nitroxide Coupling Chemistry. Journal of Polymer Science Polymer Chemistry Edition, 51, 1024-1028, 2013.
- **Aydin M.**, Tasdelen M. A., Uyar T., and Yagci, Y., In-situ Synthesis of A_3-type Star Polymer/Clay Nanocomposites by Atom Transfer Radical Polymerization. Journal of Polymer Science Polymer Chemistry Edition, 51, 5257-5262, 2013.

- **Aydin M.**, Tasdelen M. A., Uyar T., and Yagci, Y., Polymer/Clay Nanocomposites through Multiple Hydrogen-bonding Interactions. Journal of Polymer Science Polymer Chemistry Edition, 53, 650-658, 2015.

Publications:

- Barlas F. B., Ag Seleci D., Ozkan M., Demir B., Seleci M., **Aydin M.**, Tasdelen M. A., Zareie H. M., Timur S., Ozcelik S., and Yagci, Y., Folic Acid Modified Clay/Polymer Nanocomposites for Selective Cell Adhesion. Journal of Material Chemistry B, 2, 6412-6421, 2014.